THESIS FOR THE DEGREE OF LICENTIATE OF ENGINEERING

Interaction Between Graphene Derivatives and Asphaltenes in Crude Oil and Crude Derivatives

Thesis Work no: ACE 2020-0155

At Department of Architecture and Civil engineering
CHALMERS UNIVERSITY OF TECHNOLOGY
Gothenburg, Sweden

By
Govindan Induchoodan

Supervisor: Jan Swenson
Examiner: Eva Olson

Abstract

The chemistry of crude oil (SARA) and crude derivatives, and the percentage of asphaltene can vary significantly depending on external and internal factors such as the source and method of SARA extraction. If graphitic materials are introduced into a system such as SARA, it becomes an additional variable to a complex multi-phase colloid. Within the framework of this thesis, we focus on the phase stability and particle interaction between graphene and asphaltene in order to optimise the process of tailoring the microstructure of graphene embedded SARA systems, such as bitumen, to improve the gas barrier and thermal conductivity. We use various characterisation techniques in this thesis to observe the phase behaviour and the impact of embedding graphene derivatives such as GO to crude derivatives. Phase separation and agglomeration, within the SARA subfractions, were the main focus. The observations and results from the studies prove that GO is detrimental to the structure and functioning of SARA. After this observation, we attempted and succeeded in producing an fGO, that was able to overcome the challenges put forth by GO. The fGO formed stable structures, with other molecules in SARA.

Appended Paper

1. Graphene embedded bituminous roads: A new look into the design of complex nanocomposites, 2018, G. Induchoodan, B. Adl-Zarrabi, J. Swenson, L. Tang, NanoCon-18, 10TH ANNIVERSARY INTERNATIONAL CONFERENCE ON NANOMATERIALS - RESEARCH & APPLICATION (NANOCON 2018 (R)) 107-112, ISBN: 978-808729489-5

2. Detrimental effects of graphene oxide on the function of asphaltene nanostructures. 2020, G. Induchoodan, J. Swenson, submitted to ACS Energy and Fuels.

3. Co-surfactant behaviour of asphaltene and its role in stabilizing functionalized graphene micelles. 2020, G. Induchoodan, J. Swenson. In manuscript.

Publications not included

1. Tailoring polymer nanocomposite microstructure by controlling orientation, dispersion and exfoliation of GnP in LDPE via extrusion flow, 2016, G. Induchoodan, R. Kadar. Annual Transactions of the Nordic Rheology Society -16

2. Particle Emission and Dispersion Test for the Early Planning Stage: New and Advanced Wear Measurement Technique for Characterization of Environmental Impacts of Roads, (2019), G.Induchoodan, B.Ebharimi, B. Adl-Zarrabi. Euro Asphalt Euro Bitumen 2020.

Contribution Report

1. My contribution to the study includes conceptualization, methodology, validation, writing - original draft. I prepared the samples and performed the rheological measurements and SEM. The paper was written by Jan and me. It was edited by Jan, Bijan and Luping.

2. My contribution to the study includes conceptualization, methodology, validation, writing - original draft. I performed all the experiments except TLC-FID. The manuscript was written by Jan and me. The raw materials for this study were obtained from outside suppliers. The samples for this paper were prepared in-house by me. We performed a total of 4 experiments: SEM-EDX, XRD, TLC-FID, and FTIR.

3. My contribution to the study includes conceptualization, methodology, validation, writing - original draft. The paper is written by Jan and me. The raw materials for this study were obtained from outside suppliers. The samples for this paper were prepared in-house by me. The results were compared against a model, for interpretation of data. We performed a total of 4 experiments: SEM, DLS, rotational rheometer, and FTIR.

Content

List of Abbreviation

- ASTM - The American Society for Testing and Materials
- ATR - Attenuated total reflectance
- BO - Base Oil
- CCC – Critical clustering concentration
- CII – Critical Instability Index
- CMC – Critical micellization concentration
- CNAC – Critical nano-agglomeration concentration
- CPC – Complex polymeric colloid
- CXO - Cyclohexanone
- DBSA – Dodecyl benzenesulfonic acid
- DMF - Dimethylformamide
- DLS – Dynamic light scattering
- DRIFT – Diffuse reflectance infrared Fourier transform spectroscopy
- DSR - Dynamic Shear Rheometer
- EDX - Energy-dispersive X-ray spectroscopy
- fGO - Functionalised graphene oxide
- FTICRMS - Fourier-transform ion cyclotron resonance mass spectrometry
- FTIR - Fourier transform infrared spectroscopy
- GnP – Graphene nanoplatelet
- GO – Graphene oxide
- IMF – Intermolecular force
- NAs – Nano agglomerates
- NMP - N-Methyl-2-Pyrrolidone
- NMR – Nuclear magnetic resonance spectroscopy
- PAHs - Polycyclic-aromatic core
- PP – Parallel plate/ plate-plate
- rGO – Reduced graphene oxide
- SARA – Saturates, Aromatics, Resins, Asphaltenes
- SEM - Scanning Electron Microscopy
- SS2P – Synthetic Sara 2 Phase
- SS3P - Synthetic Sara 3 Phase
- THF – Tetrahydrofuran
- TLC-FID -Thin-layer chromatography flame ionization detection
- XRD - X-ray diffraction

List of Figures

1. Introduction

There is overwhelming anthropological evidence that humans have always had an affinity for augmenting their engineering capabilities. Enhancing the physical properties of their tools is the most prominent evidence in this direction. This understanding of human nature is so embedded in the idea of evolution that human history was named after the most advance material of the era such as stone-age, iron-age and bronze age. In an eccentric manner, this remains the course of human scientific evolution. An outcome of this human behaviour was the birth of composites. Composites are a class of material that is a hybrid. By definition, a composite is a physical blend of two or more materials. This blend could comprise of metals, ceramics or polymers. One could go as far as to say that today humanity exists in a composite-age. As human curiosities go, every possible opportunity has been utilised to combine various materials with one another. With the discovery of graphene in the dawn of the millennium, this material became no exception to the rule. Researchers across the globe are attempting to realise the potential of the graphene as a material and as a part of composites. This meant that it is a natural and unavoidable question to ask oneself the potential of graphene in tandem with the most significant transport infrastructure materials such as bitumen. Bitumen is a colloid that is derived from petroleum. This colloid is used in more than 70% of the global transport infrastructure and as a sealant in piping, due to its hydrophobicity.

1.1. Scientific question

In organic compounds, the macroscopic properties are often tied to the bonds formed between the various atoms [1]. The collective effect of all possible bonds is averaged over the size of the material, causing them to appear as the properties of the said material [2]. This means that if a solid understanding of the microscopic behaviour of a material can be scaled up, in effect a considerable amount of information can be extracted and predictions about the material can be made [3]. The scientific question presented here is to study the ability of graphene to coexist with dissimilar nanoparticles in a complex-polymeric-colloidal system (CPC/SARA systems). The practical application of the answer to this question would help engineers to understand methods to utilise the material properties of graphene.

This research does not attempt to enhance the rheological properties of the colloidal systems, suggest directions for researchers, discuss the potential of the material or provide solutions to scientific problems that are discovered by the industry. The sole intent of this research is to display the outcome of the interaction of dissimilar particles experimentally. By focusing on the chosen path, all energy can be dedicated to answering questions that are rarely discussed. As mentioned before, the hope is that the microscopic study can contribute to the pursuit of material enhancement.

1.2. Hypothesis

The research begins with a hypothesis that graphene or graphene derivates abrogate the colloidal structure of the polymeric system. On a molecular scale, materials interact with each other constantly [4]. The interaction can be attraction or repulsion. Molecules are in a constant struggle to reduce their free energy, and the consequence of attraction and repulsion is an attempt of the molecules to fulfil this requirement [5]. Thus, it is reasonably safe, to begin with, an assumption that one of the two interactions are occurring with the introduction of graphene or graphene derivatives in a polymeric colloidal system and that the outcome of the interaction could eliminate the colloidal structure.

1.3. Method

The method of study is a window into the mind of a researcher. This makes every research unique. Since the scientific question is independent of the engineering application, it allows this research to be conducted from an unbiased perspective. The motivations and plans are discussed in detail in **chapter 4**.

In brief, this method is more reliable to provide a step by step understanding of the potential interaction mechanism. We begin with an assumption, and then we attempt to proving/disproving the hypothesis presented by us. We work with a hope that this will bring our work one step closer to providing researchers and engineers with the knowledge to interpret the outcome of the incorporating graphene in complex polymeric colloidal systems or the idea of introduction of dissimilar nanoparticles in a system.

1.4. Narration of thesis

The thesis is divided into 6 chapters. The idea of each chapter is to study the hypothesis systematically. **Chapters 2-3** will discuss and establish an understanding of the CPC system and the nanoparticles. In **chapters 4** the experimental method and expected outcomes are discussed, following which a discussion into the results is conducted in **chapter 5**. Finally, in **chapter 6** the future outlook of this research will be presented.

In the start of every chapter, a philosophical idea is presented to orient the readers. The idea presented in the introduction of every chapter is the scaffolding over which the narration of the chapter is set.

2. SARA systems

In predictive science, it is essential to understand the structure of a system under study to predict the behaviour arcuately. This means comprehending a structure-function relationship in a system, through understanding the underlying mechanism, governing principles, origin and evolution of the system. This was famously coined by Francis Crick in his axiom, ''If you want to understand the function, study the structure'' [6]. From the perspective of this thesis, this means that the structure-function and the underlying working principles of the parent material must be established [7]. A visible example of this theory is the human hand. The fist may be multifunctional, but its primary functions are for fine-controls and power movement. The structure of an opposing thumb makes fine-controls possible, and the ability of the fingers to touch the thumb makes grabbing possible and though this, power movements. On a molecular scale, the chemical structure of the molecule determines its properties and the properties of the molecule determine its function. By this principle, the structure-function of the molecules in bitumen must be understood to be able to determine its structure-function. Only then will it be possible to predict the enhancement required in the structure to attain the intended function [8]. Although it is possible to perform such a study on all the molecular families in bitumen, in reality, this would be a colonial undertaking that would be inefficient on an engineering scale. The reasons for this will be discussed further in the thesis. For now, it is essential that a simple structural design of the bituminous system can be established. This will enable us to setup a basis that is required to commence a structure-function study of bituminous systems. One location to search for such a simple design of bitumen is in the parent material from which it is derived, petroleum.

2.1. Petroleum

Petroleum is defined as all naturally occurring hydrocarbon [9]. By definition, petroleum includes hydrocarbons that occur in all states of matter, in its pure or mixed form and with or without heteroatoms such as oxygen, nitrogen and sulphur [10]. This includes bituminous systems. Hydrocarbons are molecules with a carbon backbone [11]. The length, orientation and the atoms bonded to the backbone will determine the properties of hydrocarbons [12]. This includes the boiling point and the state of matter of the hydrocarbon. Most often, when petroleum is extracted from its source, it comes in the form of a complex array of hydrocarbons. This is often called as crude [9]. Amongst others, the most widely used system to extract various petroleum fractions is by the process of fractional distillation [13]. In this process, crude is heated to evaporation, and the vapours of crude are condensed. It must be noted that it is allowed for different hydrocarbons to have similar boiling points. Hence, various hydrocarbons, in crude, can be categorised into petroleum fractions based on the boiling point [14]. Thus, when crude vapours condense, they do so at various stages. These petroleum fractions can have hydrocarbons with varying carbon numbers, bonds and heteroatoms [15].

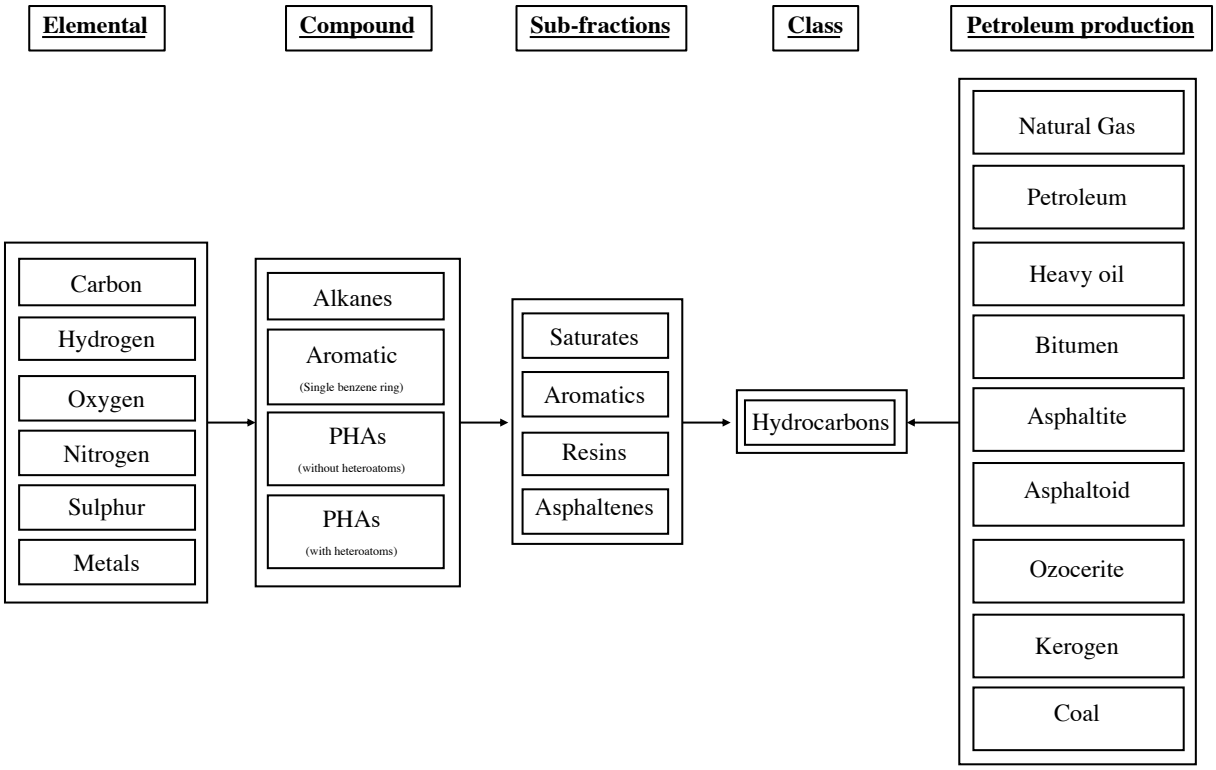

Figure 2.1: - Global clart of the subdivision of hydrocarbons; All hydrocarbons are divided into elemental composition; The elements arrange themselves to form alkanes and aromatics of different architecture; These organic molecules can be arranged into 4 fractions called SARA. All petroleum derivatives are a combination of these fractions [5].

2.2. Petroleum and petroleum derivatives

Petroleum has a carbon-based structure, with an elemental composition of carbon, hydrogen and heteroatoms such as oxygen, sulphur and nitrogen, Figure 2.1. These elements arrange themselves to form linear alkanes, branched alkanes, cyclic alkanes, monoaromatic and polyaromatic analogies [16]. The hydrocarbons mentioned above also bond with the heteroatoms to form compounds such as thiols, pyridines, ketones and many more. Based on the source and the probable structure of the condensed hydrocarbons, these hydrocarbons can form constitutional and stereoisomers leading to 10s of thousands, if not 100s of thousand structural possibilities for each increase in carbon number. Due to this, it can be challenging to determine the properties of individual hydrocarbons in crude [17]. The array of structural design would be vast and nearly impossible to categorise. Thus, petroleum can be more naturally divided into broader fractions, based on their nature, origin or a characterisation technique, refer to Figure 2.1. Such classification includes acidity, polarity, molecular weight and solubility [9].

- If petroleum was to be divided based on the family of hydrocarbons. Petroleum can be divided into alkane family, aromatic family of aromatic hydrocarbon without heteroatoms (polarisable aromatics) and aromatic family of polar compounds [9].

- Another method to categorise petroleum fractions is based on its stability and solubility of various hydrocarbons in liquid hydrocarbons [18]. In petroleum science, solubility is not defined as the molecular solvation of a solute but rather the ability of the solute to not precipitate in a solvent [20]. Through this process, petroleum fractions are categorised into alkane hydrocarbon insoluble and soluble fraction, see Figure 2.2. The categorisation is done by standard provided by The American Society for Testing and Materials (ASTM).

A combination of these two techniques leads to the standard method of SARA fractionation of petroleum [18]. This is famously called as SARA [9]. SARA is an acronym for Saturates, Aromatics, Resins, and Asphaltenes. This method is a two-stage division of petroleum into polarised and polarisable components of crude. In stage-I saturates, aromatics and resins are seen being the alkane soluble fraction and asphaltenes being the alkane insoluble [15]. On stage-II, the extracted fractions are divided into its corresponding hydrocarbon family of alkane family, aromatic family of aromatic hydrocarbon without heteroatoms (polarisable aromatics) and aromatic family of polar compounds. Petroleum derivatives such as crude, heavy oils, bitumen and petroleum solids can be classified as a combination of the 4 SARA fractions at various ratios [16], refer to Figure 2.1.

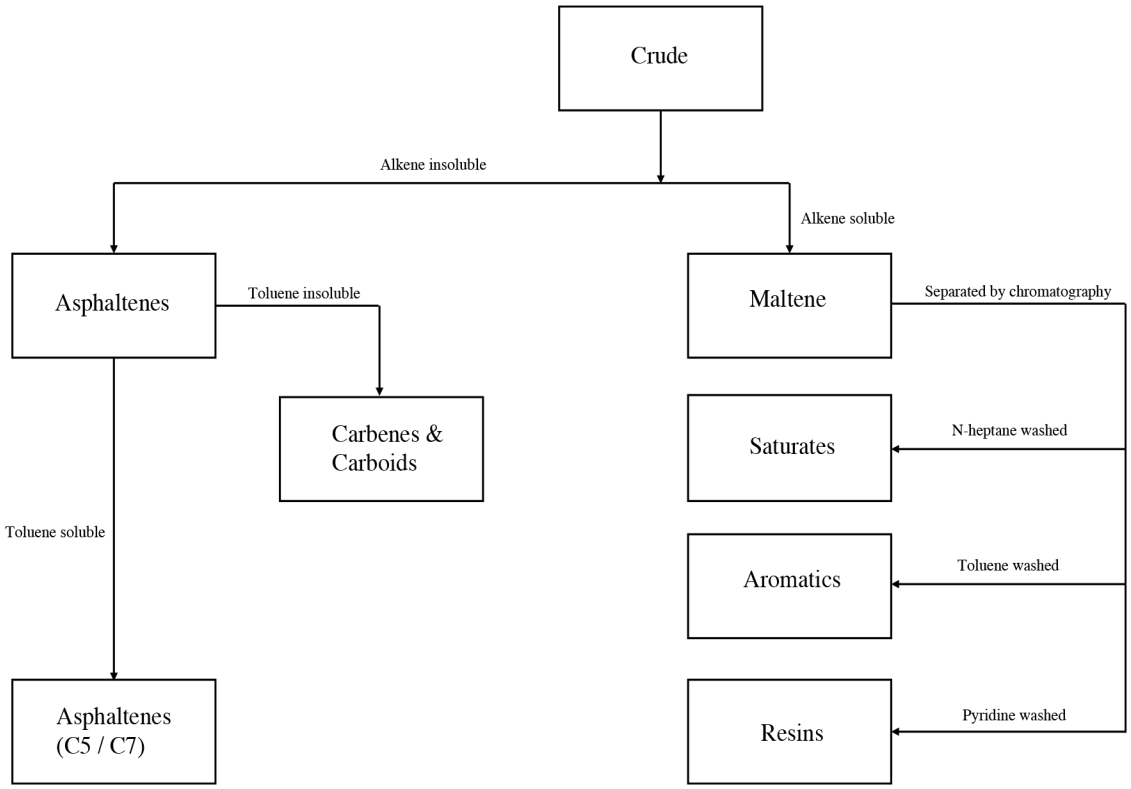

Figure 2.2: - ASTM D 4124-01 method of separating SARA fractions from crude, heavy oil and bitumen. The crude is separated into alkene soluble and insoluble. The alkene used here is most often n-heptane. The soluble fraction is called maltene. Maltene is separated into its constituent fractions through chromatography into saturates, aromatics and resins.

2.3. SARA fractions

SARA is an analysis method that divides crude oil components according to their polarizability and polarity [09]. Asphaltenes are the toluene soluble n-heptane insoluble fraction, while aromatics, resins and saturates together form the n-heptane soluble phase called maltene, see Figure 2.2. In the earlier days, maltene was assumed to be a homogenous fluid. It was later, by the method of chromatography, that maltene was further divided into different fractions based on the polarity and polarizability [19].

2.3.1. Asphaltenes

Asphaltenes are the fraction of crude that gives it the characteristic colour and provides bitumen with its behaviour. Asphaltenes exist as nano-solids of 2 nm in size in ambient conditions. Molecular orbital calculations [20] and mass spectroscopy [21] studies indicate that the chemical architecture of asphaltenes is that of a polycyclic-aromatic core (PAHs), with condensed aromatic units making up less than 20% of the structure. The majority of the structure is an alicyclic and open-chain aliphatic, with alkanes existing in the form of end-functionalised structures, which is expected to cover nearly 55% of the structure. The heteroatom count in asphaltenes is displayed to be the highest in the petroleum fractions, and hence the core of asphaltene has a high number of CHO, CHOS, CHNO and CHNOS molecular series with an average H/C ratio of 1.75 and C/O ratio of 0.15. FTICRMS (Fourier-transform ion cyclotron resonance mass spectrometry) indicates that asphaltene has a short range of condensed aromatic units with the majority of the aromatic cores having a count of 10 to 20 carbon atoms [22].

2.3.2. Resin

Resins are polar aromatic structures in crude [10]. Resins are observed to be semisolid while observations also indicate that resins too can be observed to be a black solid-like substance at room temperature. Resins are speculated to have a fused aromatic core of 2-4 fused rings with indications that resins could have a complex aromatic structure similar to asphaltenes. It is postulated that resins have a similar composition to asphaltenes, with some resins demonstrating higher polarity than asphaltenes. Resins are generally found to contain fewer heteroatoms. In high viscous petroleum derivatives such as bitumen, a sizable portion of the low-oxygen and hydrogen-deficient molecules are resins. Resins are of interest in scientific studies and production of petroleum derivatise due to their peptizing behaviour. In the mass spectroscopy studies, resins have shown to comprise of the largest condensed aromatic structures in petroleum derivatives such as bitumen. This accounts for roughly 50% of its chemical architecture. They have a density of nearly 1.07 g/cm^3 at 20° C [20, 21].

2.3.3. Aromatics

Aromatics, also called Naphthene-Aromatics, is the polarizable fraction of crude. Unlike resins and asphaltenes, aromatics are more compounds with single benzene rings of 10 to 30 carbons. Aromatics are a mixture of the paraffinic-naphthene-aromatic solution with heteroatoms such as sulphur and an average aromatic ring number of 2.6. They have a density close to 1 g/cm^3 and often found as yellow to red liquid, at room temperature [20, 22].

2.3.4. Saturates

Saturates are giving rise to a colourless or lightly coloured liquid in crude. They consist of alkanes hydrocarbons, in paraffinic-naphthenic form. They are apolar, form the lightest fractions of petroleum derivatives, with a density of nearly 0.9 g/cm^3. In SARA systems such as bitumen, the glass transition of the saturate fraction is most dominant. They have almost no heteroatoms. The saturate fraction consists of nonpolar materials, including linear, branched, and cyclic saturated hydrocarbons. Saturates exhibit a glass transition temperature at -70° C [20, 22].

2.4. Colloidal structure of SARA

Over the years, many proposals for the microstructures for petroleum and petroleum derivatives have appeared [23]. It began with hypothesising Asphaltene were free carbon suspended in a maltene solution [24]. After this era, a large group of researchers subscribed to the postulate of a sol-type and gel-type material. The first asphaltene models relied on the Tyndall effect (Tyndall effect is light scattering by particles in a colloid or a very fine suspension.) [25]; later models relied on the viscoelasticity [26]. Sols and Gels were differentiated based on their elastic response to loading. In the 1970s, a new idea was developed based on the flocculation model of crudes [27]. In the model, they studied main influencing components that determine the behaviour of SARA — concluding to be asphaltenes and the surfactants. In the study, the entire maltene was categorised into one homogeneous liquid and considered as one influencing unit. During the same era, Yen et al. [28], proposed a new microstructure for crude and bitumen. The new model integrated a micelles-colloidal microstructure. This later came to be known as the Yen-model. Over the years the Yen-model has been modified to accommodate for recent scientific findings. Proposed by Oliver C Mullins, the iterated version of Yen's model later came to be known as the Modified-Yen-Model [29], see Figure 2.3.

To understand the Modified-Yen-Model and the colloidal structure of crude, heavy-oils, and bitumen, the formation of the micelles and its suspension in the solvent must be understood. Critical concentrations are a crucial step in understanding the formation of microstructures. If asphaltene micelle formation in crude is analogous to polymer

liquid crystals in solvents [30], the free energy of the system that determines the phase stability, behaviour and ordering of the particles is influenced by concentration, entropy, molecular dimensions of particles and solvent, orientation, amongst others [31, 32]. Due to the complexity of the asphaltene molecular architecture, the early manifestation of the micelle formation can be inferred from the volume fraction in the crude.

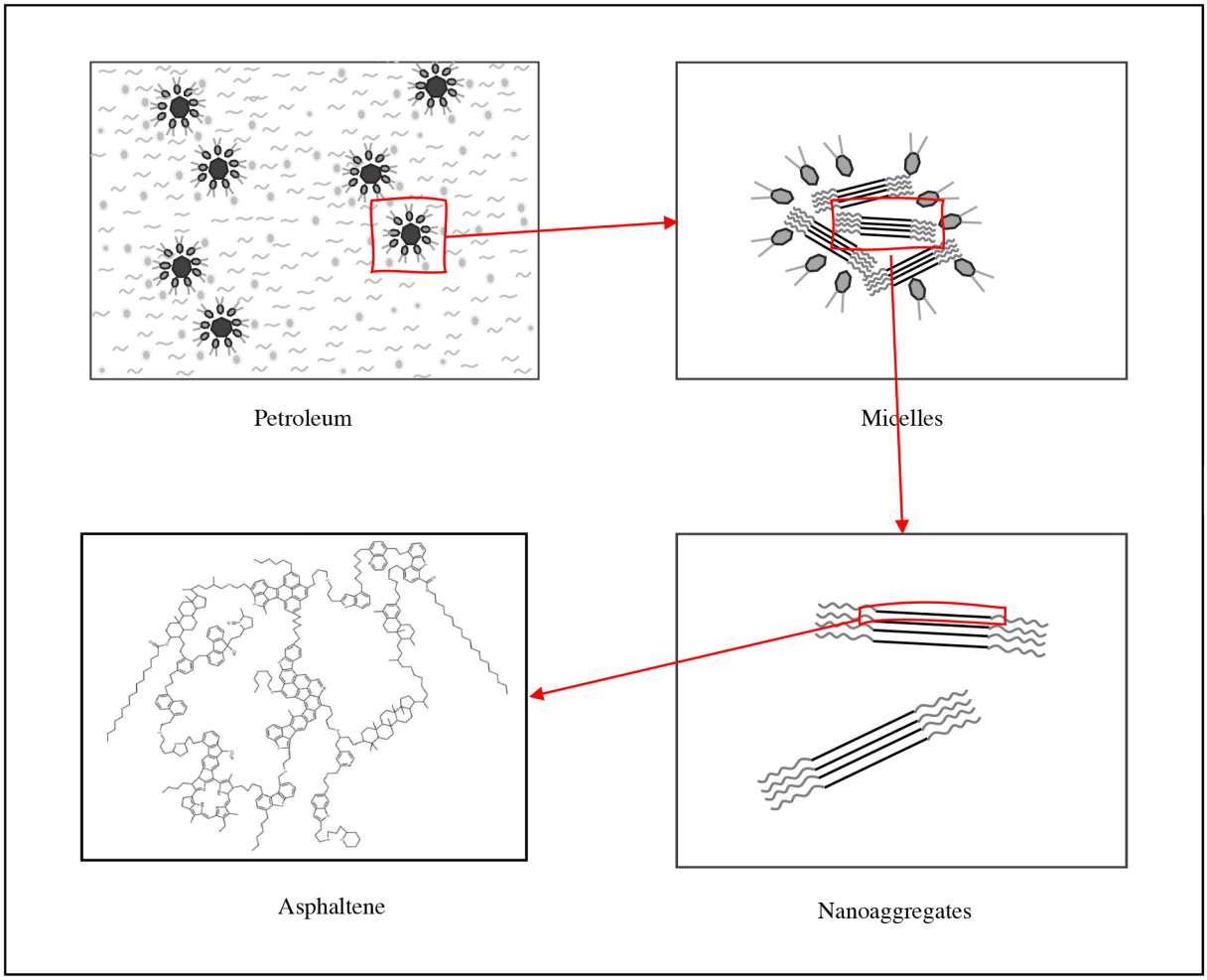

Figure 2.3: - The postulated colloidal structure of crude (top-down). A). Polar Micelles are suspended in a paraffinic-naphthenic-aromatic solution. B). The micelles are formed by asphaltene clusters in the core and resins acting as surfactants. C). Asphaltene clusters are formed when asphaltene nano aggregates interact with each other in an aromatic solvent. D) One of the many proposed architecture for asphaltene molecules present at the core of the micelles.

2.5. CNAC (Critical Nano Agglomeration Concentration)

As discussed earlier, asphaltenes are found to have a surface-activated heteroatomic-poly-aromatic architecture at the core (PHAs). This means that asphaltenes can have active functional groups present in the polyaromatic core. This chemical structure of asphaltene causes it to have multiple intermolecular forces (IMF) present in the core [33]. These include hydrogen bond, dipole moment, van der Waals forces and π-interactions. Aromatic cores have an electron-rich π-system [34]. This can lead to the electrons interacting with the π-systems of other aromatic molecules to form a type of

non-covalent interaction called the π-effect [35]. In asphaltene, this would mean that the molecules will self-interact to form stacks or agglomerates of asphaltenes [36, 37, 38]. These asphaltene rich phases are formed early in the stage of petroleum and are the preferred state of asphaltene molecules, and they are referred to as nanoaggregates. A single sheet of asphaltene molecule is postulated to have a molecular weight of ~750Da, and a nanoaggregate is estimated to be a stack of 10 molecules [22]. The concentration at which asphaltene molecules self-associate to form nanoaggregates (NAs) is called the critical nanoaggregate concentration. Beyond the size of NA, steric hindrance from the other feature of asphaltenes, i.e. the aliphatic sidechains, dominate. This limits the growth of the stacks. Since the resin molecules have an aromatic core, it is not unlikely for resin molecules to stack with the asphaltene molecules [39].

2.6. CCC (Critical Cluster Concentration)

As mentioned above, when the structure of asphaltene restricts further growth, the rapid growth of NAs hinders. Ideally, the formation of NAs stops after most of the conversion of asphaltene into NAs. Still, when the concentration of asphaltenes exceeds ten times that of what is required to form NAs the NAs themselves interact to form clusters. These clusters are only sterically bond to each other. The range of concentration, when this happens, is called the critical cluster concentration. There are uncertainties around the actual size and scale of cluster formation. That said, it is highly supported that these clusters are fractal, and unlike NAs in clusters, the binding energy is found to be rather small, leading to conclude that they are not formed by the crosslinking of the aromatic cores. This phenomenon is due to the clusters being susceptible to change in the free energy of the colloidal system. The influencing factors are temperature, solvents, or an increase in cluster concentration. At higher temperatures or shears, it would lead the clusters to disassociate. It could also lead to phase separation in petroleum, causing the clusters to flocculate [40].

2.7. CMC (Critical Micellization Concentration)

Critical micellization concentration is the concentration above which surfactant molecules self-associate to form micelles in a solvent. A surfactant is a class of molecules that are amphiphilic. One part of the molecule is lipophilic, and the other is hydrophilic. Surfactant class of molecules interact at the interface between two surfaces such as water-oil or water-air to lower their energy state. In a pure solvent such as water, the surfactants tend to remain as monomers below the CMC. At the critical concentration, the surfactant monomers reduce its interfacial energy and self-associate to form micelles. The shape, size and other characteristics of the micelles are dependent on surfactant-solvent interaction and the presence of a co-surfactant. During the reduction of the interfacial energy, the micelle achieves to segregate of the hydrophilic/lipophilic moieties. Factors such as the hydrophilic-lipophilic balance, polarity of the solvent, volume fraction and self-assembly mechanism can lead the

micelle to self-assemble to form spherical, globular, spherocylindrical, hexagonal, planar or bilayer structures. More than often the micelles evolve with change in free energy of the system. The change in free energy can lead to surfactants having more than one CMC in a solvent [41].

Polar-aromatic molecules, such as resins, act as a surfactant. Asphaltenes would interact with the polar head of the resin molecules to form micelles. The lipophilic end of the resin molecule would extend outwards into the paraffinic-naphthenic—aromatic solvent in crude. The resin molecules behave similar to a peptizing agent, forming inverse micelles in an apolar solvent such as crude. The heteroatoms and the polar heads of both the species, i.e. asphaltenes and resins, exert IMFs through hydrogen bonding and dipole-dipole moment. The volume fraction and the chemical structure of the resin molecules will determine the interaction of resins with NAs. At low volume fractions, resins will adhere on to the surface of NAs, but might not be able to involve in peptizing NAs flocculates [22].

2.8. CII (Critical Instability Index)

On a macroscopic scale, CII helps equate the stability of petroleum from the ratio of the SARA fractions. The stability of the colloidal structure is assumed to be a delicate balance between the ratio of the sums of saturates and asphaltenes to the sum of resins and aromatics, see eq. 1. If the petroleum has a CII below 0.7, it is generally considered as a stable. When the CII value is above 0.9, the colloidal structure in petroleum will destabilise. This number has significant implications for the underlying mechanisms and interactions that maintain a stable colloidal structure. The various scenarios can lead to the stabilisation or destabilisation of the structure [42]. For instance, Asphaltenes are solvable in toluene, xylene and other aromatic structures. The increase in aromatic content in petroleum will help form a stable dispersion in saturates. This leads to a ‘’bridged’’ structure of resin peptized clusters and supported by NAs dissolved in aromatics. When CII is low, it indicates that the asphaltenes are stabilised by dispersion in aromatics.

$$CII = \frac{Asphaltene + Saturates}{Resins + Aromatics} \tag{01}$$

If the volume fraction of asphaltene increases, it could lead to larger clusters forming and them interacting with each other in the crude. With the increase in the size of the clusters, complete or partial phase separation of the petroleum will occur. The consequence of this is seen as fouling in crude pipelines and sedimentation in bitumen. Resins can also cause destabilisation of the micelle structure. If two segments of resin are partly absorbed on two different clusters, it could lead to the bridging of both the clusters causing them to come together despite the potential existence of electrical repulsion. Another mechanism for resins to destabilise the micelles is when the absorbed resin molecules have an opposite charge to that of asphaltene, which clusters. This can be seen in particular for larger sized clusters.

It is well established in polymer suspensions that there is a direct relation between the minimum depth of the secondary minima and the volume fraction of the suspension, which indicates that the higher the volume fraction, the lower the minimum depth of the secondary minima to initiate weak flocculation [43]. If there is a reduction in the entropy of the resin molecule at approach towards the asphaltene and the adsorption energy of the pair is not sufficient to compensate for this reduction, it could lead to an osmotic pressure outward from the asphaltene molecule, squeezing the resin out from asphaltene leading to a creation of a depletion zone outside the cluster. This too will make the cluster to undergo weak flocculation [43]. An Increase in the saturate content leads to a shift in the free energy of the system, leading the polar and polarisable fractions to destabilise and disperse in petroleum. This too could lead to phase separation of the microstructure.

3. Graphitic Structures

Disproving existing theories is believed by many to be the forefront of science. In 2018, a GPS satellite launched into orbit around earth by NASA lost its planned orbital motion causing the satellite to go into an elliptical orbit around earth. Dr.Pacome and Dr.Sven used this mishap as an opportunity to retest the values of general relativity through gravitational redshift. The intention was not to reprove a 100-year-old theory but to observe deviations. For the researchers, the deviations in the value would display the missing link in general relativity, helping them further advance the theory. This is an excellent example of the strive for the truth that every researcher fights to attain. The most important lesson from this is that science advances from accidents and coincidence. This was also the case with graphene back in 2004. Andre and Kostya frequently held 'Friday night experiments' - sessions where they would try out experimental science that wasn't linked to their day jobs. One Friday, the two scientists removed some flakes from a lump of bulk graphite with sticky tape. They noticed some flakes were thinner than others. By separating the graphite fragments repeatedly, they managed to create flakes that were just one atom thick. Their experiment had led to graphene being isolated for the very first time. The material was theorised to be non-existent due to the energy configuration of the theorised material. It was precisely this question that the team of researchers from Russia and Brittan disproved, and as they say, the rest is history.

3.1. Graphene

Graphene is an atomic layer of linearly arranged benzoinated structure of carbon [44], see Figure 3.1. It has an sp2 hybridised orbital in the bulk, this orbital configuration would suggest an σ-bond in the bond axis with two lobes of a delocalised π-bond. As a consequence of this delocalised π-orbital, the crystal is flat [45]. At the edge of the crystal structure of graphene, it has an sp3 hybridised orbital [44]. The benzoinated structure also means that crystals have a tendency to agglomerate in solvents [46]. The definition of a crystal in this context must be differentiated from the concept of crystalline carbon. A carbon crystal is an in-plane isotropic structure of carbon atoms with long range order, while a crystalline carbon is a synonym for diamond [47].

The electron dynamics of the crystal can be best described by the relativistic Dirac equation [48]. By this, the Fermi velocity of the electrons in the crystal is replaced by the speed of light and hence the effective mass of the electrons vanishes, making them appear as massless fermions [49]. This lets graphene to have quantum anomalies such as the quantum hall effect [50], absence of localisation [51] and ballistic transportation [52]. Up to several microns thick, graphite is a semi-metal, but the lack of bandgap around the Fermi level of graphene makes the material metallic in nature at a smaller scale [53]. A zero-band gap implies that the valance band and conduction band of graphene overlap, allowing the electrons to hop in energy between the bands

and be able to move around freely [54]. This leads to the ever-popular properties of the material and simultaneously limits its electronic, optoelectronic and semiconductor application [55].

Pristine graphene has an optical transmittance of 97.5% with 0.01% reflectance [56]. This behaviour decreases as stacking increases. Graphene has a surface energy of 18.77 eV, between the six-carbon structure [8]. This is even higher than that of the Helium atom, which is 18.6 eV. This means that during relaxation of both graphene and the colliding atom, the colliding atom will relax faster and be repelled back from the surface. It could be said in other terms that graphene's hexagonal structure has a very high electron density that will not let any molecule pass through it. Due to the structure and size of pristine graphene, the crystals are near chemically inert and insoluble in many organic solvents [57]. This limits the application of pristine graphene. As an alternative, graphene is chemically or physically modified to suit the application. This type of graphene is categorised as a graphene derivative.

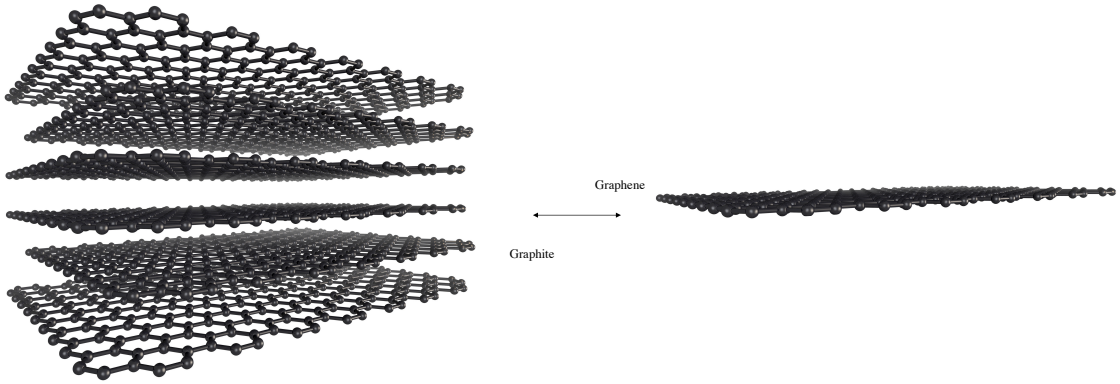

Figure 3.1: - Graphite to graphene, structural difference. While graphite is a stacking of atomic layer thick graphite, graphene is a single crystalline sheet of carbon. Image purchased from adobe photo stock.

3.2. Graphene derivatives

Graphene can be seen as a simple starting configuration for many carbon structures. For example, graphene monolayers can be stacked to form graphite, rolled in to form nanotubes and wrapped to form buckyballs. Due to the sacristy of natural graphene and high cost for monolayer graphene in the current market, low cost/ ample volume alternatives such as graphite nanoplatelets, GO, reduced GO, and functionalised GO are usually considered. All these structures of graphene are widely used in research for various purposes or as a precursor for various applications. In this research, we have used multiple graphene derivatives [58].

3.2.1. Graphene nanoplatelets

Graphite nanoplatelets or GnP are usually a few layers thick. They contain multiple layers of atom-thick carbon sheets. This is a reasonably inexpensive alternative to

pristine graphene as it provides similar surface conditions on a large scale. As mentioned in **session 3.2**, the thickness of GnP makes it opaque. It could also contain edge-defects depending on the production method. GnP is also of interest to many researchers as it is used in labs to extract graphene layers from it by using various exfoliation techniques, see Figure 3.2. GnP also provides a good understanding of the macroscopic configurational and orientational order of the particles in a matrix [59].

3.2.2. Graphene Oxide

GO is a metastable derivative of graphene with induced defects [60]. The defects are induced by incorporating oxygen into the pristine chemical structure. This transforms the bulk of graphene from an sp2 hybridised to an sp3 hybridised state. Oxygen and carbon bond to form epoxy bridges and hydroxyl groups in the bulk and pairwise carboxyl groups on the edges, with islands of monoatomic thick graphitic domains. The introduction of oxygen transforms the planar structure of graphene [61]. There are many existing and competing models for the transformed structure. It can be contemplated that the oxygen functionalities act as an energy barrier for graphitic domains from stacking [62]. This change in the chemical structure causes GO to lose many of the desired properties of graphene [61]. For example, these changes cease GO to be inert. As a consequence, GO is reactive and polar. This means that the GO can form hydrogen bonds and dipole moment in aqueous and organic solvents.

It has been observed that GO remains in 2D form only in solvents and on top of substrates [63]. The monolayer dispersibility of behaviour of GO is observed in basic and neutral solvents such as water and alcohol. In acidic solvents, GO flocculates to trigger phase separation. When dispersed on a substrate, GO is in an interface between the surface of the substrate and air. This too causes GO to retain its 2D structure, see Figure 3.3. In solvents GO interacts with the surrounding solvents to form a uniform dispersion. The solvent-GO interaction is favourable when compared to GO-GO interaction. This is true for concentrations of GO below CMC [30]. Above the limit, GO can interact to form structures such as colloids and agglomerates. It has been observed that GO remains in 2D form only in solvents, and the monolayer dispersibility of GO is observed in basic and neutral solvents [46]. In acidic solvents, GO flocculates to trigger phase separation [46]. Researchers also state that the process of self-association of GO is influenced by dispersive hydrophobic forces, which are the largest contributors for GO to self-assembly [63]. The dominant role to self-assembly is by the entropic component of the free energy of self-association of amphiphilic nanoparticles [64]. The authors also state that above CMC the loss in the orientational component of the entropy is compensated by the translational entropy. It is also seen that colloidal GO deposits at low pH and high ionic strength of solvents. Therefore, the stability of the colloidal GO is a balance between a long-range repulsion, caused by the electron double layer interaction, and a short-range attraction [46]. In solvents, the theoretical solubility of GO is predicted to be around 23 $(MPa)^{1/2}$ [65].

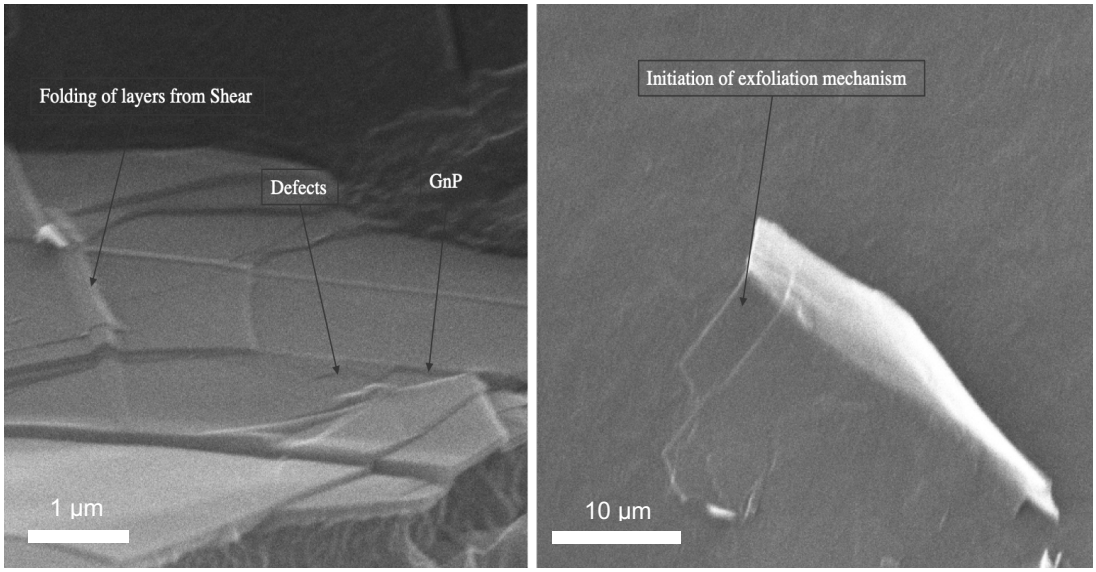

Figure 3.2: - a) Graphene nanoplatelets on polymeric substrate. It can be seen that GnP has structural defects. Due to in situ shearing of GnP in polymeric melt, GnP folding of sheets takes place. b) The exfoliation is non-uniform and a few layers thick by in-situ exfoliation.

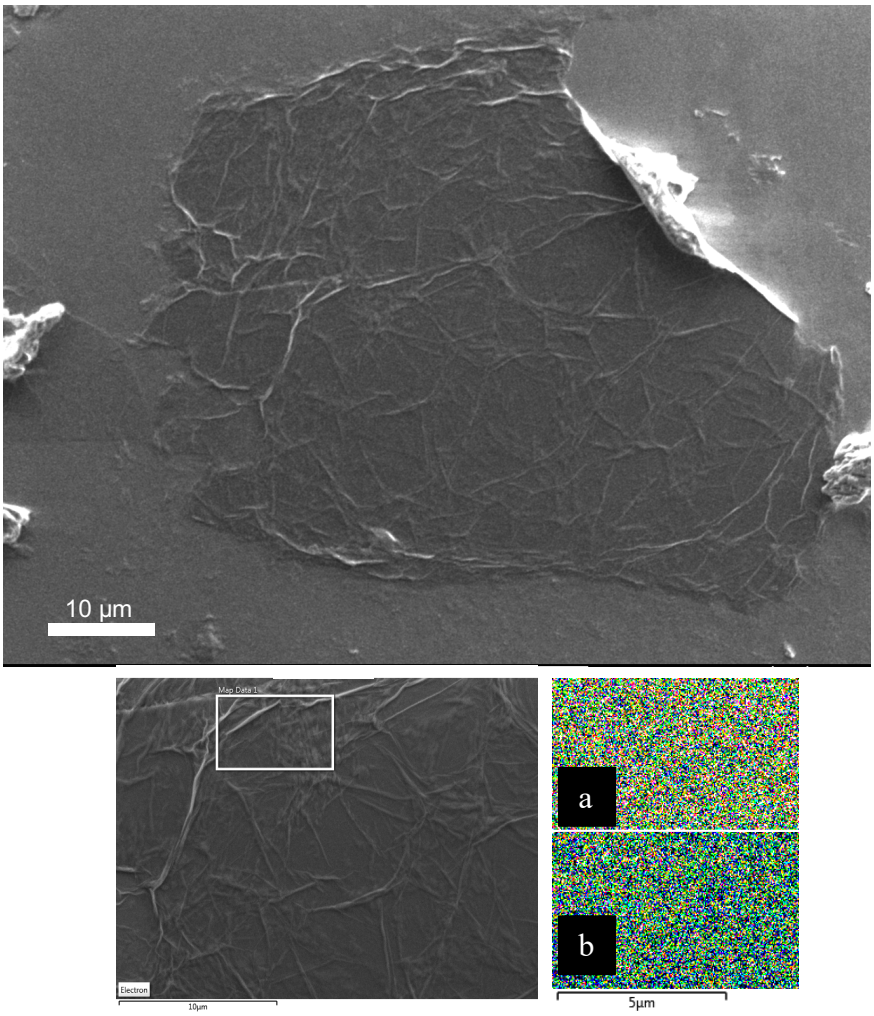

Figure 3.3: - GO on a silicon substrate under SEM. Below, Zoom in view of the GO sample. a) EDX scan of oxygen. b) EDX scan of carbon

3.2.3. Functionalised Graphene Oxide

Functionalization of GO is a method of modifying the chemical functionality on the surface of GO. This is achieved by replacing the oxygen functional group with another electroactive species. The functionalization can occur with covalent or non-covalent bonding [66]. Covalent functionalization includes nucleophilic and electrophilic functional groups and non-covalent bonding mostly include the bonding of cations, anions or hydrogen to a π-electron on the surface of GO [67]. The type of functional species and its characteristics would vary the behaviour of the GO sheet. In principle, the selection of the functional species depends on the application of GO. In Figure 3.4, a flowchart has been presented to illuminate the possible functionalisation strategies.

3.2.4. Reduced Graphene Oxide

GO is a metastable state of graphene. When elevated to higher temperatures or over time, these oxygen functional groups can decompose to return graphene to an SP2 hybridized state. The reduction of GO to rGO can also be achieved through chemical reactions and electrical process. When this happens, the oxidized functional groups are removed, to obtain a graphene material. This form of graphene is called reduced GO, often abbreviated to rGO. rGO usually contains more defects and is of lesser quality than graphene produced directly from graphite. Although in theory, reduction of GO must provide graphene, it is not the case, rGO contains residual oxygen and other heteroatoms, as well as structural defects [68].

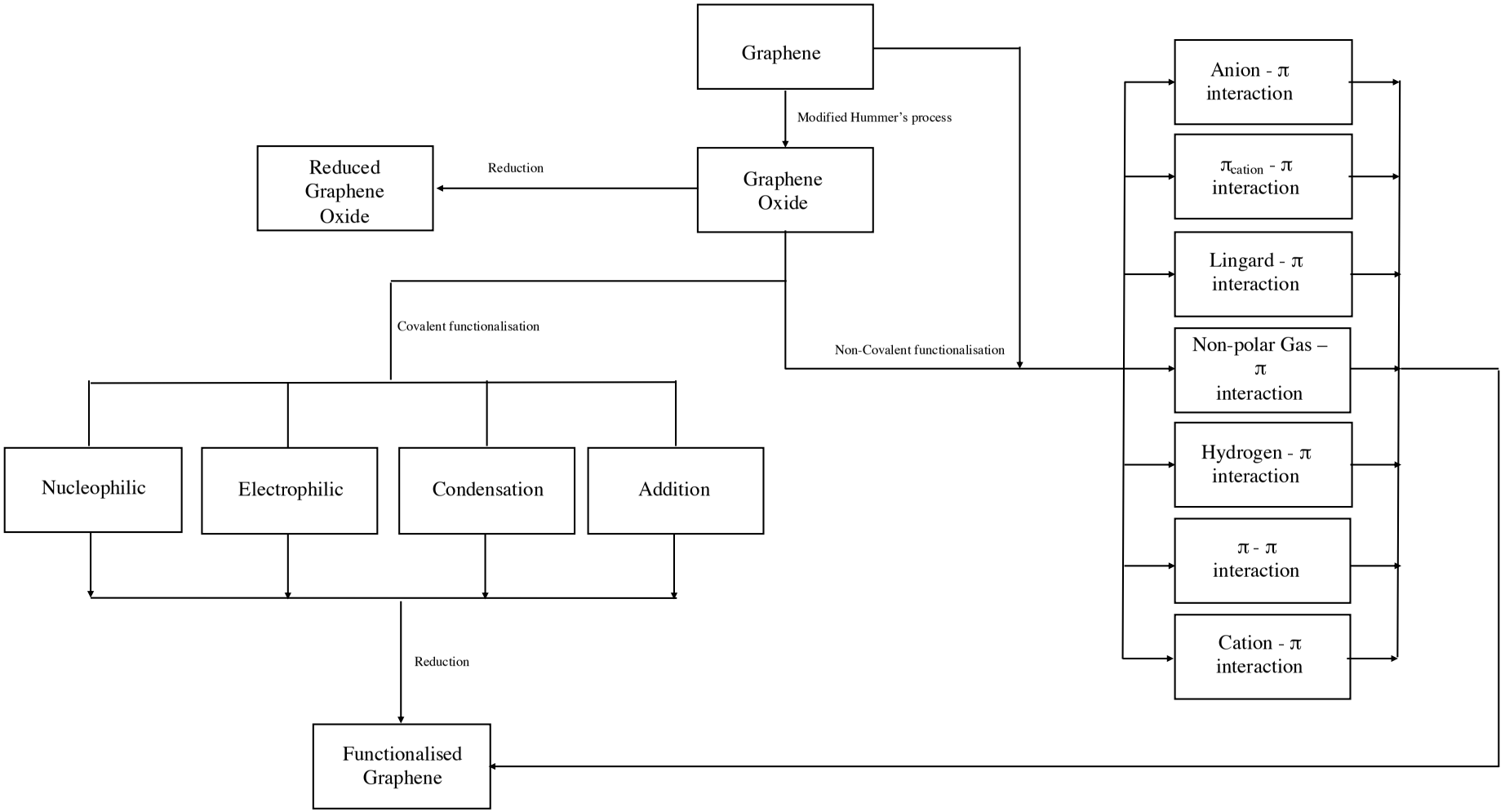

Figure 3.4: - Flowchart about the strategies of graphene functionalization oxidation and reduction. Graphene can be directly functionalized through non-covalent methods by utilizing the pi-electron interaction. Graphene oxide can also be oxidized through the modified hummers method and then covalently functionalized with specific species depending on the application.

4. Experimental Planning and Methods

In 1980, while presenting his famous TV show ‘The Cosmos’, Carl Sagan put forward his aphorism that ‘’Extraordinary claims require extraordinary evidence’’. This statement later came to be known as Sagan Standard. His statement was part of a more vital philosophy called ‘the burden of proof’. The burden of proof or *Onus Proband* in Latin is the philosophical idea about the responsibility of a disputant in an argument to provide evidence for their position. Often misconstrued as a requirement for positive stance, the concept spans to negative and null stance too. A positive statement is often seen as the shortest path to overcome the burden of proof, e.g. If someone intends to prove a claim that there exists a chair in the building, the person needs to find just one chair in the building to be proven right. In such situations, claims can be broad, global and unspecified. On the other hand, to prove a claim that a building has no chairs, one would have to be extremely mindful of their claim as the chances of being disproven increases. This causes the disputant to be vigilant, meticulous and rigorous in formulating and presenting the claim. To remain glued to the claim the disputant will be forced to reiterate the statement multiple times, redesigning or reimagining the statement until the statement can be modified no further that the person is forced to abandon the negative claim.

In the start of this chapter, we make such a contrary claim. The research begins with the hypothesis that graphene derivatives, such as GO, will negatively impact the stability of the colloidal structure of SARA. In this chapter, we would assume the role of the disputant and the audience. We would then argue for and against our work until we reached a consensus. By doing this, the above claim will be systemically put to the test and experimentally disproved until the disputant is forced to abandon the claim and accept the possibility for the contrary.

4.1. Experimental preparation

4.1.1. Benchmarking experimental investigation

In material characterisation, when a characterisation technique is utilised, there are standard steps that are followed in order to benchmark and calibrate. The calibration happens over three stages [69]. Step 1: Zeroline, Step 2: Baseline, Step 3: Standardised material and Step 4: Sample. For example, in calorimetric experiments, the sapphire crystal would be considered as standard material [70], and similarly, in small-angle scattering, silver behenate would serve the purpose of an experimental standard [71]. These steps will be discussed in later sessions. The intent of introducing the concept of benchmarking is to discuss its importance in scientific work [72]. Benchmarking a procedure helps researchers gain better understating of the unknown substance under study. By this, unknown-unknowns, unknown-known and systematic

errors can be reduced in studies [73]. This concept transcends beyond material characterisation and into systematic scientific studies in general. To understand the workings of a complex multi-phase system, such as graphene derivative in SARA, a simple and clear understanding of the system should be established. Such an attempt is made in this thesis through a series of 3 papers.

4.1.2. Isolating Asphaltene interaction.

Although the thesis intends to encompass the SARA in general, the primary area of application of the results is in a heavier fraction of SARA. The natural conditions of such heavy SARA fractions must be taken into account. For instance, conditions such as temperature and viscosity. At low temperatures, the viscosity of SARA fractions such as bitumen is exceptionally high, as shown in **paper 1**. Such high viscosities make it unlikely to observe a phase separation at a low temperature, as the high viscosity will counteract the flocculation. However, a high viscosity does not exclude the possibility of agglomeration.

Graphene derivatives have high aspect ratios, so at high viscosities, the graphene derivatives can likely fold, intercalate and form sterically bound agglomerates, like an onion structure [74]. To overcome the formation of such undesirable structures, in SARA, it is desirable to reduce the viscosity or increase the temperature. Asphaltene-resin micelle stability has been displayed to be a factor of temperature, and graphene derivatives, such as GO, are thermally unstable at temperatures above 150° C [75]. Furthermore, at such high-temperature GO reduces to form rGO. SARA will also be oxidised, leading to an increase of the asphaltene fraction [76]. Thus, there are many complexities in utilising a naturally occurring SARA, and it is essential to keep the temperature at the same constant value in all studies for a valid, meaningful comparison. A variation of the ratios between the components in SARA can lead to a direct instability of the colloidal microstructures, see **section 2.8**. Even without added nanoparticles, a CII-value above 0.9 would lead to oxidation, which causes the SARA system to flocculate, see **section 2.8**. The agglomeration initiated by added nanoparticles would be challenging to observe and reproduce in such an environment. This, in turn, is the motivation for extracting asphaltene from SARA derivatives and studying synthetic systems.

4.1.3. Asphaltene in Organic Solvent

Asphaltene in an organic solvent is a binary phase. In this, asphaltene is dispersed in a carefully selected organic solvent. In such a system, the asphaltene remains in the NAs state after its CNAC [77]. In this binary phase system, NAs are expected to be stable, emulating the aromatic-NAs interaction in SARA. When the asphaltene concentration exceeds approximately ten times its CNAC concentration, a limit called critical clustering concentration; asphaltene must form clusters, see **section 2.5.** Some

studies refer to this as asphaltene cluster [10], but for the better distinction, it will be called colloids. To be able to design such a system, the IMFs that dictate the dispersion quality of asphaltene in solvents must be understood. In **paper 2**, a detailed discussion on the interactions in colloidal asphaltene is presented.

To summarise, a comprehensive subject review and calculations made it evident that solvents such as THF, toluene, xylene, CXO and cyclohexane are good-solvents for asphaltenes [78], and THF, water and NMP are good-solvents for GO [79]. While this knowledge is useful, there is another requirement. Both GO, and NAs must be able to disperse in the same solvent. This condition is necessary since it is only under such a condition that it is possible to study flocculation caused by molecular interactions.

THF fulfils the criterion mentioned above [78, 79]. In THF, GO coagulates in forms of compact or open clusters [46]. When the concentration is above the critical concentration; this could lead to flocculation of these large coagulated structures. Thus, the solvent-GO interaction is more energetically favourable than the GO-GO interaction, only below the critical concentration of GO.

4.1.4 Asphaltene in Oil

The ternary phase system (SS3P) was designed to replicate the behaviour of NAs and resins in its micelle form [80]. In SARA, NAs are dispersed in a paraffinic-naphthenic-aromatic solvent. In saturates, i.e. alkanes, the NAs form micelles through peptization by resins, see **section 2.7**. Alkanes are bad solvents for asphaltenes, see **paper 3**. Due to this, asphaltenes will not interact with saturates, causing sedimentation. Therefore, resins are introduced to the asphaltene-saturate binary system. Resins interact with asphaltenes, through peptization triggering micellization. The mechanism for this was introduced in **paper 2**.

In SS3P, the CMC behaviour of NAs-Resin micelles is isolated. In general, when the surfactant concentration exceeds the CMC, the previously monomeric surfactant molecules will reduce its interfacial energy and self-associate to form micelles [81]. A surfactant is a class of molecules that are amphiphilic in nature, i.e. they have lipophilic and hydrophilic moieties. Due to this nature surfactants tend to be located at the interface between two surfaces such as oil-water or air-water to lower their energy states [82]. The shape, size and other characteristics of the micelles are dependent on the surfactant-solvent interaction and the presence of a co-surfactant [83]. In solvents, the surfactants can exist as isotropic structures. This changes at higher concentrations when they can form long-range ordered structures. Factors such as the hydrophilic-lipophilic balance, polarity of the solvent, partial volume fractions and assembly mechanisms influence this mechanism and can lead to micelles forming a spherical, globular, spherocylindrical, hexagonal, planar or bilayer structure [83]. More than often, micelles evolve with change in free energy, causing them to have more than one CMC.

As discussed in **chapter 2,** resins are a family of molecules similar to asphaltenes. Although resins can be recovered and reused from the SARA system, through the process of chromatography, the molecular structure of the recovered resin will remain chemically complex. When such a chemically complex structure is introduced to asphaltene, the interaction mechanism and the bonding strength cannot be predicted with precision. This means that a coherent microstructure might also be unpredictable, and furthermore difficult to determine experimentally. Thus, resins were replaced by other candidates [84]. 4-Dodecylbenzene sulfonic acid (DBSA) is amongst them. DBSA is an acid of linear sodium dodecylbenzene sulfonate. It is an alkyl aryl sulfonate with a hydrophilic sulfonate acid and a lipophilic dodecylbenzene [85]. The SS3P system is utilised in both **paper 2** and **paper 3**.

4.2. Sample Preparation

As discussed in **chapter 2**, asphaltenes are a family of molecules that exist in SARA. By the process of chemical extraction, asphaltene can be extracted from SARA systems. The standard method for chemical extraction is provided by ASTM [18]. The protocol for asphaltene extraction provided by ASTM was utilised in **paper 2** and **paper 3**. N-heptane was used as the chemical of choice for the extraction, as the target molecule is C7 asphaltene. The other subfamilies of asphaltenes are C5 and C3 [10]. The extracted asphaltenes are obtained as black solids, see Figure 4.1. These are agglomerates that flocculated during the extraction of C7 asphaltene. Later these particles were dispersed in toluene at a concentration of 5 mg/ml, see Figure 4.2. The dispersed asphaltenes were studied by transmittance bright field imaging to observe the stacking of individual particles. As seen in Figure 4.1, these are, in fact, obtained as NAs and not asphaltene molecules. The extracted NAs are studied in more detail in **paper 2**.

The NAs are dispersed in various solvents to understand the dispersibility, refer to **section 4.1.3**. Following this, the SS2P and SS3P systems were produced as per the protocol designed in **paper 2**, see Figure 4.3. The dispersibility of asphaltene was as predicted by its solubility parameter [86]. Asphaltene was seen to disperse in CXO, THF and toluene while remained phase separated in DMF, methanol and ethylene glycol, see Figure 4.3. 3 SS2P systems were created using different organic solvents. DMSO, toluene and THF were chosen. It was discovered that THF was most suitable for the study. Although GO is soluble in toluene up to 0.00157 mg/ml, it is significantly lower than the asphaltene, which has a dispensability of 10.5 mg/ml [87, 88]. This is a magnitude difference in the order of 4. Thus, THF was chosen as the best solvent for this experiment. The GO used in this study was produced by the modified hummers method [89]; the procedure is discussed in **paper 2** and **paper 3.** The method we used to produce fGO in **paper 3** has been discussed in the same paper.

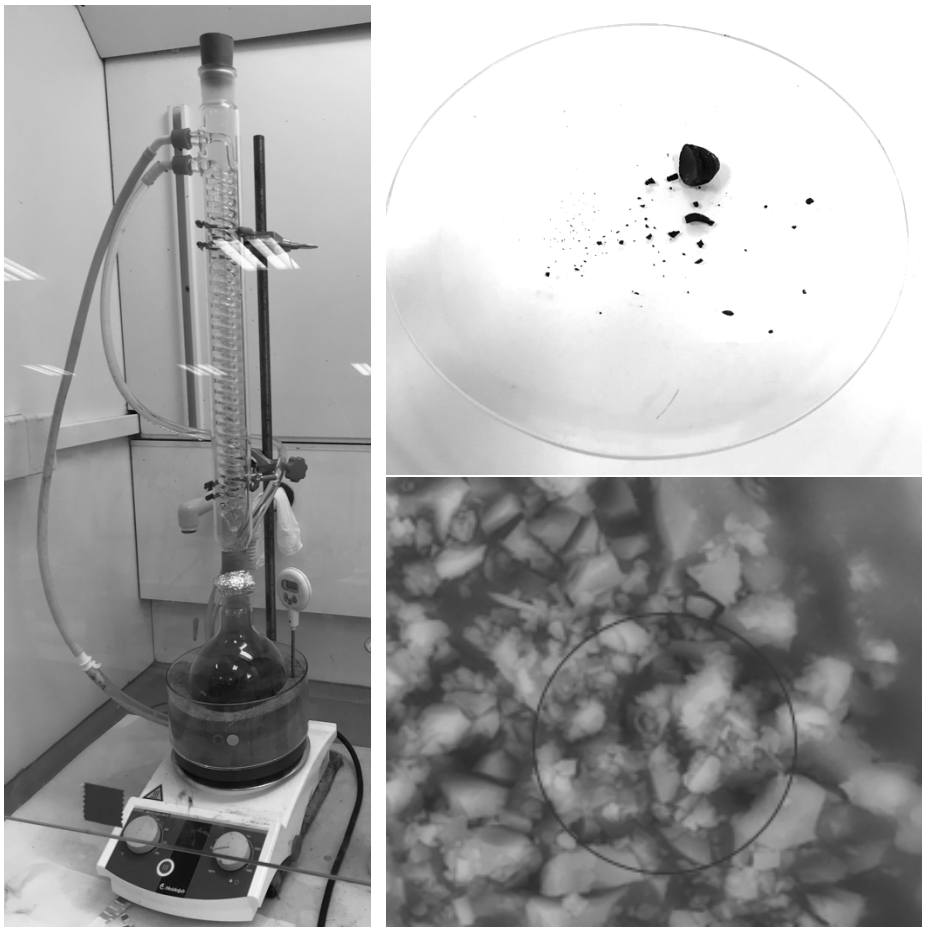

Figure 4.1: Left: Chemical extraction of asphaltene from SARA; Right-Top: asphaltene particles after chemical extraction from bitumen; Right-Bottom: extracted asphaltene under electron microscope. (see **paper 1**)

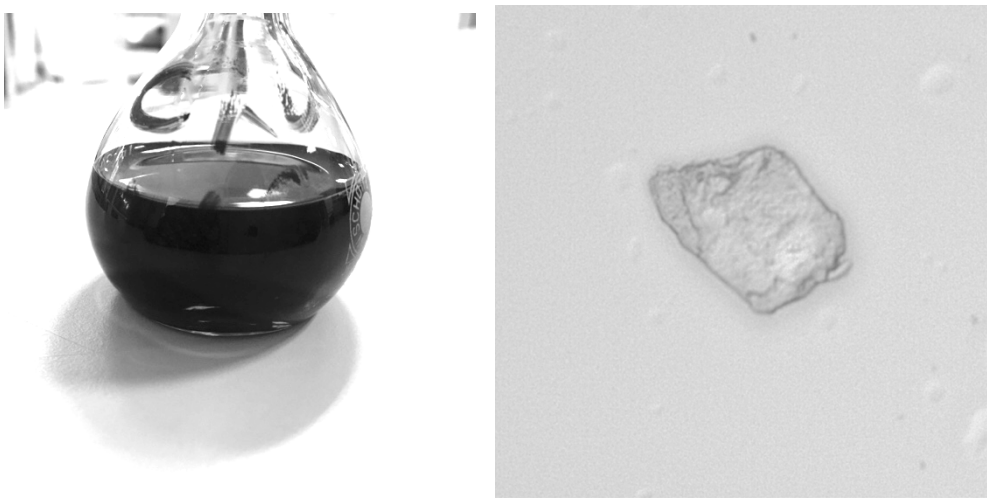

Figure 4.2: Left: asphaltene dispersed in toluene at a concentration of 5mg,7ml; right: dispersed asphaltene particle under bright field imaging.

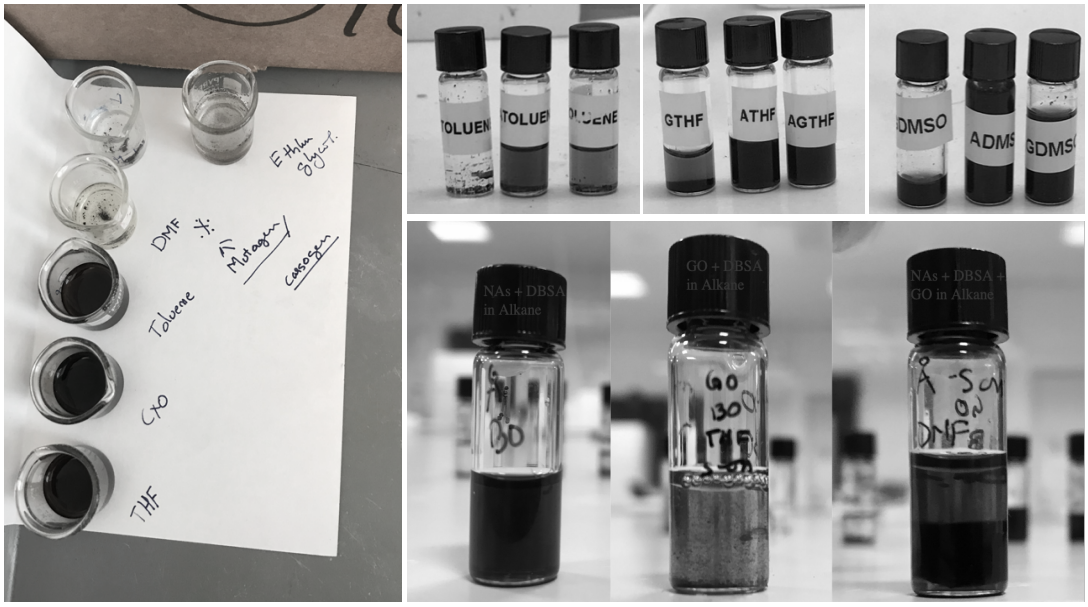

Figure 4.3: Left: Asphaltene dispersed in various solvents; Right-Top: SS2P system of GO, NAs and GO+NAs in toluene, DMSO and THF; Right-Bottom: SS3P system with NAs, GO and NAs+GO.

4.3. Characterisation techniques

Characterisation techniques utilised in this thesis can be categorised into microscopy, spectroscopy, diffraction and rheology. The characterisation techniques were selected based on its abilities to provide information about the interaction behaviour of graphene derivatives and SARA system. For the validation of results, complementary techniques were used. Figures of merit are conditions set by the scientific community to produce standards and results that can be reproduced and reused by researchers around the globe [90]. Thus, any technique used must comply with the figures of merit. The techniques used in this thesis can be divided into qualitative and quantitative methods [91]. To conduct a holistic study, the researcher often chooses complementary techniques and a blend of qualitative and quantitative techniques to attain acceptable results.

4.3.1 Scanning Electron Microscope

In science, there exist not many techniques by which researchers can directly observe their samples. Most, if not all, techniques are an interpretation of the response of the instrument. In such techniques, the results are merely a numerical response from the interaction between the instrument and the sample. This is not the case in imaging. While philosophically imaging is no exception to the earlier interpretation, on a macroscopic scale, imaging provides direct information of the sample at hand. This is the reason imaging was chosen as the first technique of characterisation. In **paper 2**,

SEM is used to observe the microstructure. While we used the same technique to observe particle size in **paper 1** and **paper 3**

In microscopy, an incident beam of energy source made to bounce off the surface of a sample [92]. The beam is then recorded and processed to produce an image. The beam can be reflected by the sample or transmitted through the sample. In the later, the detector is placed on the opposite end of the instrument [93]. In methods such as SEM, the energy source is the electron.

The limitation of microscopy is that the technique does not provide information about the material beyond the visible information [94]. The chemical composition, behaviour and response to extrinsic factors such as hygro-thermal, rheological and mechanical loading cannot be determined. Techniques such as SEM are often complimented using spectroscopy techniques such as EDS [93].

The main advantage of microscopy is that it shows the structure of the material. While human eyes can observe information at 100 μm, a powerful enough microscope can go down to 10^{-10} m [92]. This is the range of Transition electron microscopy. In this study, such a resolution was not used. Instead, the measurements were performed at a magnification between 10^{-3} m to 10^{-7} m. This is the range of a Bright field to SEM.

As shown in Figure 4.4, an SEM has an electron gun, electron optical system and electron analyser. The electron gun can be a high energy source of electrons; this source can be tungsten-hairpin (T-h), a LaB_6 source or a field emission source (FES). While the source has an energy spread of 3 eV, the FES source has a range of 0.3 eV [92]. Rayleigh resolution is a major limiting factor for microscopy studies. It is the smallest distance at which two objects can still be resolved as being separated. Thus, the resolution limit (r) of a microscope is proportional to the wavelength (λ) and the numerical aperture.

$$r = \frac{0.61\lambda}{NA} \tag{02}$$

So, for a bright-field microscope, the resolution highly depends on the source of light, which is between 0.4 μm and 0.7 μm [92]. In SEM, one could describe the source with the de Broglie resolution, with approximating the resolution to be about 1 nm for 30 kV [93]. An advantage of SEM when compared to other microscopes is its ability to maintain a depth of focus. The depth of focus is the ability of the instrument to maintain a focus across a field of view, regardless of the surface roughness. The region of effective focus is called D. It is within the plane of optimum focus and

$$D \approx \frac{2r}{\alpha} \tag{03}$$

Where α is the beam divergence, so, this is maintained by either reducing the magnification of the divergence angle.

Surfaces of samples have multiple electron ranges, i.e. auger electrons, secondary electrons, backscattered electrons. Following this, there lie characteristic x-rays and continuum x-rays. It could be said that interacting with different kinds of regions will provide different radiation. The information retrievable from each region is proportional to the atomic number, angle of incidence and accelerated voltage.

In SEM, the two primary electron regions used in interaction are with backscattered and secondary electrons. While the former is used to attain compositional contrast, the latter provides topological contrast. Secondary electrons are low energy electrons.

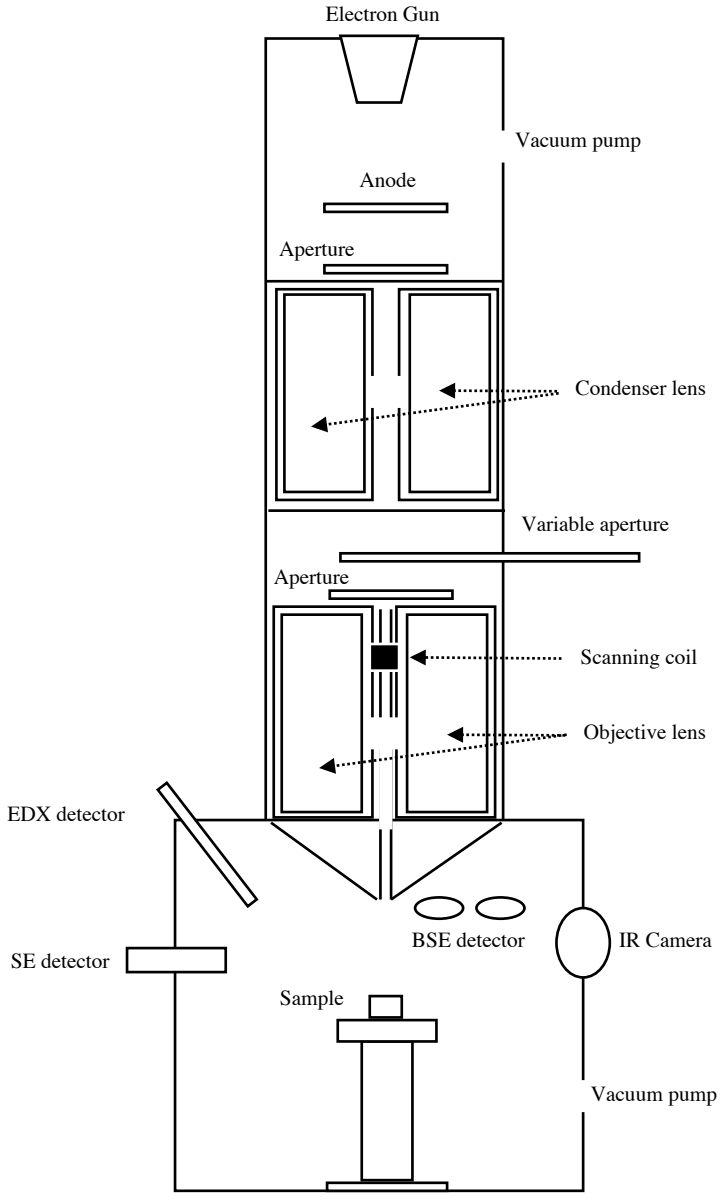

Figure 4.4: Schematic representation of a SEM instrument.

Surface chemistry can cause a potential barrier for secondary electrons, and surface morphology can lead to absorption of secondary electrons. Depending on the atomic number, the number of backscattered electrons varies, they are directly proportional. This type of elastic scattering is independent of accelerated voltage, unlike secondary electrons [93].

For this study, SEM is needed to attain close imaging of the larger structure of the particles. In the case of asphaltene, graphene and GO, Raman imaging is a powerful tool to study the phase variation of the surface of the nanoparticle [95]. A phase mapping of the sample will help attain information about the thickness, defects and structural anomalies.

4.3.2 Fourier Transform Infrared Spectroscopy

After i). oxidation of graphene into GO, ii). functionalisation of graphene and iii). extraction of asphaltene, FTIR was used as a tool to identify the functional groups present in both **paper 2** and **paper 3**. For graphene FTIR was used to understand the functionalities of GO. In the case of asphaltenes, FTIR was used as an indicator to identify the class of asphaltene. Doing so will help isolate the parent source and origin of the crude.

Vibrational spectroscopy is a potent tool [96]. The results from such techniques provide information about the molecular structure, bonds, functional groups, compound length, degree of crystallinity and contaminations. Thus, most often, it is used as a rapid tool to analyse organic compounds. The technique generally has three modes of function, transmission, ATR and DRIFT. Depending on the characterisation output, state of matter and thickness of the sample, the appropriate mode is selected.

Samples used in FTIR characterisation are required to be ''active'' in order to be able to characterise them by this method [97]. This is so because the fundamental working of the technique requires a sample to contain dipole moment. By theory, a molecule with no dipole moment will not be able to absorb the infrared rays. It is well established that molecules absorb photons. In the electromagnetic spectrum, the photons in the energy range of infrared are known to be absorbed by many molecules. For organic studies, this is significant because the wavenumber of the absorbed photons corresponds to the vibrational wavenumber of the molecular bond between the atoms.

The energy source in FTIR studies is infrared light [96]. Every object radiates light in the infrared region. Infrared has a wavelength between visible light and microwave (between 1-100 microns). The primary source of infrared radiation is thermal radiation or heat. When atoms or molecules are in motion, they produce radiation. When the source of heat is higher, the motion of the atoms increases, this, in turn, generates greater amounts of radiation. Infrared spectrum can be divided into three regions: near,

mid and far. Near infrared is closer to visible light and far infrared is closer to microwave.

In FTIR, when atoms or molecules are energised, they vibrate, and these vibrations occur at fixed frequencies called natural frequencies. If a beam of photons is bombarded on a molecule, and the applied frequency of the photons is equal to the natural frequency, then the vibration of the molecule will be amplified. This vibration is analogous to spring with two atoms acting as weights and the bond that forms between the two atoms acting as a spring. Since the natural frequency of each bond is unique, the absorbed wavelengths act as an indicator of the identity of the bonds present in the molecule [98].

In a polyatomic molecule, the atomic motion can vibrate in translational, rotational and vibrational modes with 3N degree of freedom in both linear and nonlinear directions. N represents the number of atoms in the polyatomic molecule. In a molecule, the electron motion is linked to the energy transition of the electrons that are in orbital. Rotational and translational motion of electrons is characterisation techniques of its own and are out of the scope of this chapter. Bonds in vibrations can undergo vibration by stretching or bending of the bonds. The magnitude of the vibration is propositional to the amount of energy absorbed by the electrons, with stretching producing more substantial peaks than bending. Stretching of bonds leads to change in the spacing between interatomic distance and bending leads to a change in the angle between the bonds. Stretching can be both compression and extension, and bending can be twisting, rocking, wagging and scissoring [98].

However, a limitation comes in the form of dipole overlap. If two or more compounds in a mixture are analysed, all compounds can absorb the infrared rays at the same time [100]. If they absorb similar frequencies, it will, therefore, be difficult to distinguish their peaks. This is the reason why many times FTIR is combined with SEM/EDX, XPS and SIMS.

There are typically four regions. Between a wave number of i) 2500 cm^{-1} to 4000 cm^{-1}, the vibration is typically single bond. Ii) 2000 cm^{-1} to 2500 cm^{-1}, the vibration is typically double bond. Iii) 1500 cm^{-1} to 2000 cm^{-1}, the vibration is most often a triple bonded carbon and finally below 1500 cm^{-1} the region is called iv) fingerprint region or skeletal bond [96]. They are typically complicated absorption peaks, and it is difficult to assign a peak to a specific group, at this region. The information that can be deduced from the peaks includes the peak intensity, broadness of the peak and the position of the peak. If the peak transmittance is below 5%, then the absorption can be considered to be very strong while if the transmittance is nearly 95%, the absorption can be considered to be very weak.

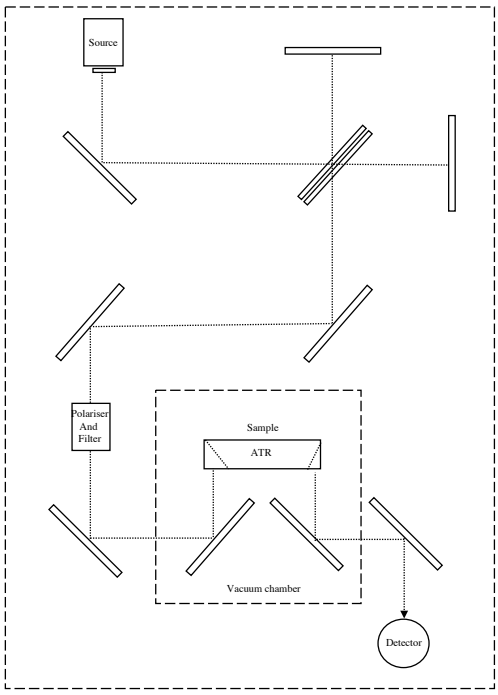

Figure 4.5: Schematic representation of a reflectance setup for a FTIR instrument.

A typical instrument has a heat source as the source of the infrared source. The light from this source is then passed through an interferometer. At the interferometer, the path of one beam of light is split into two. The two beams are later recombined. At the detector, the difference in the intensities of the two beams is measured. This measured data is in the form of a function of the difference in the path (Figure 4.5). This will allow constructive and destructive patterns to occur, allowing the user to measure the interferogram. The sample preparation for an FTIR can vary on the type of measurement. In our studies, the ATR method was used. ATR (Figure 4.6) is a form of reflectance method, with the other being transmittance. With the ATR method, the incident beam is directed towards a diamond crystal; the sample is placed on the crystal that absorbs the waves. The wave is internally reflected through the crystal back to the sample several times before it is transmitted out of the sample towards the detector [96].

The most significant peaks that are seen in FTIR measurements are C=O (1660 -1820 cm^{-1}), C-O (1000-1300 cm^{-1}), O-H (3300-3600 cm^{-1}), COOH (1170-1725 cm^{-1}) and ester C=O (1000-1300 cm^{-1}). Other include alkanes, alkenes and aromatic rings and phenol ring substitution band. Using the area under the FTIR peaks, information about the material can be understood [98].

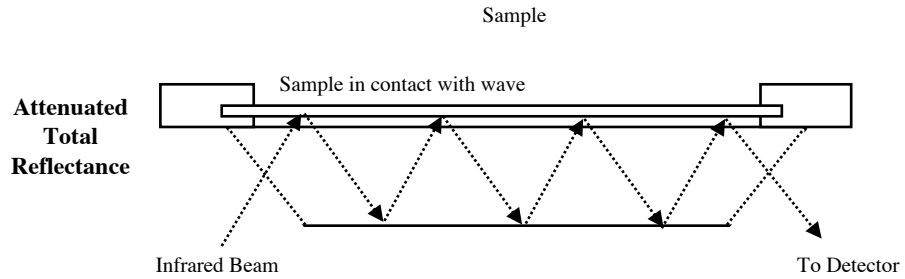

Figure 4.6 ATR setup. The incident ray is bounced back and forth between sample and the ATR crystal, before refracting towards the detector

4.3.3 Diffraction

4.3.3.1. X-ray Diffraction

X-ray diffraction is a characterisation technique that works in the principle of constructive interference [100]. In liquids and solids, the average interatomic distance is between 1-3 Å. If the structure of a crystalline material has to be determined, then the wavelength of the radiation must be similar to the spacing in the crystal's atoms [101]. X-rays fit into this criterion as they have a range from 0.1 Å to 100 Å [100]. X-rays are short wavelength electromagnetic radiation that is produced as a consequence of a deceleration of high energy electrons or by the transition of the inner orbital electrons in an atom.

Near monochromatic intense (Kα) X-rays are the most common type of radiation used in such studies [100]. The penetration depth of X-rays used in such studies is proportional to the wavelength of the source. Target metals such as Mo, Cu, Co, Fe and Cr are used as a radiation source. The X-ray released from the source is passed through carefully packed metal plates called collimator. The metal plate has a small gap that allows a narrow beam of X-rays to pass through. This narrow beam of X-rays is then bounced off a monochromator that absorbs the undesirable wavelength by allowing only the required wavelength to pass through. A schematic representation of an XRD setup is shown in Figure 4.7.

In many cases, the monochromatic X-rays have the same wavelength as the electrons in the atom. One such example is CuKα and carbon. The beam of X-rays that act as the primary source interacts with the atoms in the crystal. The energy of the X-ray that interacts with the electrons is not sufficient to eject the electrons. This interaction causes the electrons to undergo elastic scattering [102]. During elastic scattering, the electrons start to oscillate, which in turn transforms the electrons into a secondary source. The atom acts as a periodic array of for scattering. When the two wave sources interact constructively, they amplify the intensity of the final beam while the opposite causes the wave to cancel out [103].

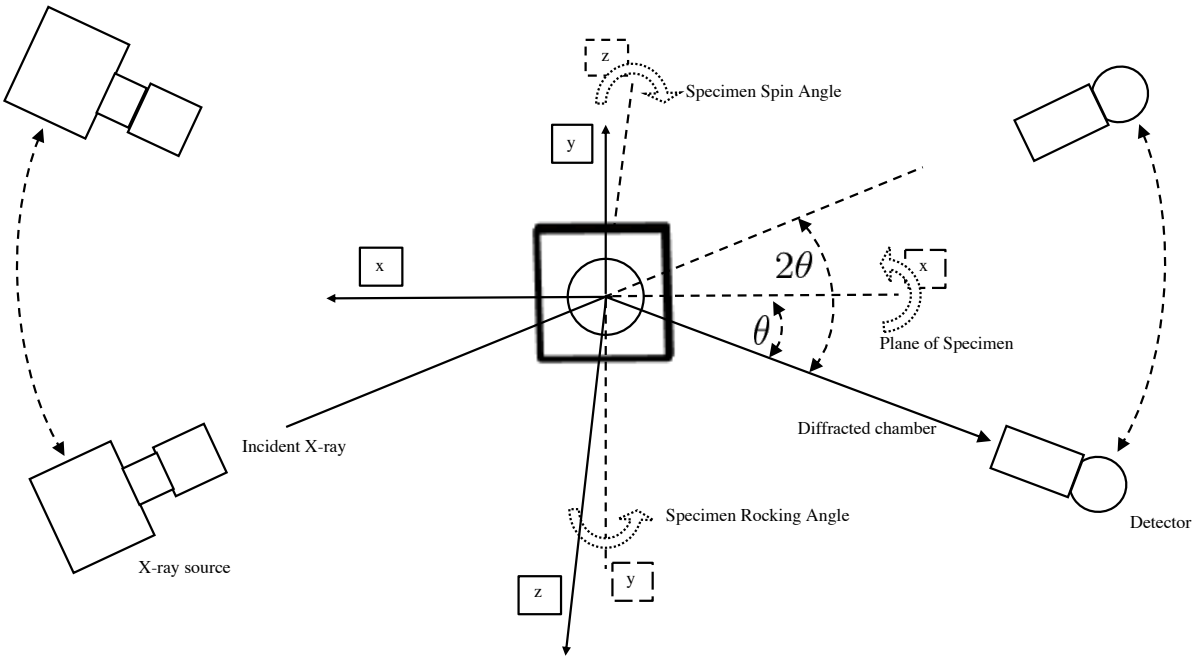

Figure 4.7: Schematic representation of an XRD setup

The XRD measurement in **paper 2** was performed using a Bruker D8 Advanced X-ray diffractometer using CuKα radiation with a wavelength of 1.54 Å. The peaks of interest are γ-peak, Π-peak and 010 peaks. The peaks are a representation of the miller indices of crystal plane. Using these the aromaticity (f_a), amorphous carbon (L_a), interlayer spacing (L_c), and crystal size (n) can be determined.

$$f_a = \frac{C_{ar}}{C_{ar} + C_{al}} \tag{04}$$

C_{ar} = Area under Π-peak.
C_{al} = Area under γ- peak.

$$L_a = \frac{1.84\lambda}{B_a Cos\Theta_a} \tag{05}$$

λ = Wavelength of X-ray
B_a = half width max of 010 peak
Cos θ_a = Cosine of scattering angle of 010 peak.

$$L_c = \frac{0.89\lambda}{B_c Cos\Theta_c} \tag{06}$$

λ = Wavelength of X-ray

B_C = half width max of Π-peak
Cos θ_C = Cosine of scattering angle of Π-peak.

Using the L_C, the average number of carbon atoms per laminate can be calculated. It corresponds to n,

$$n = 0.32\frac{L_c + (d\pi_{band})}{d\pi_{band}} \quad (07)$$

4.3.4 Rheology

Rheology is a powerful tool to indirectly observe the behaviour of liquids, colloids and viscoelastic fluids [104]. The rheological behaviour of fluids is an indication of the microstructure [22]. Changes in the microstructure can be identified by a change in the complex modulus. Another important output from rheological measurements is the time-temperature superposition.

If the rheological study utilised a rheometer, samples are usually sandwiched between two surfaces and sheared. The interpretation of the results is acquired from the shearing of the sample. During our study, we found that it is very much possible to misinterpret rheological data of opaque or colloidal systems if they are not complemented with diffraction or thermal analysis, see **paper 1**.

In a rotational rheometer, viscoelastic samples are sheared in a narrow gap between two surfaces. In the most common setup for a rotational rheometer, the bottom surface is fixed, and the top surface has a degree of freedom in two dimensions (rotational and transitional). This was the setup that was used in **paper 1-3**. With such an experiment, the viscosity and viscoelasticity of a material can be studied. Viscosity is the magnitude of internal friction in a fluid and is defined as the ratio of the shear stress and the shear rate. In a rotational rheometer, the stress is calculated from the torque and the shear rate from the angular velocity. Viscoelasticity is the property of materials that exhibit both viscous and elastic characteristics when undergoing deformation.

With a rotational rheometer, depending on the setup, the instrument can be used to perform stress-controlled or strain-controlled measurements. In the controlled-stress rheometer, the torque or stress is the independent variable that is applied to the geometry. In the controlled strain rate rheometer, the material is placed between two plates. Key factors that help measure the material properties are the geometry and dimensions of the plates. The upper geometry is attached to the driving motor spindle—the driving motor functions with an air-bearing that rotates under the conditions provided for the experiment. The geometry of these surfaces could be concentric cylinders, parallel plates or a cone and a plate. In this thesis, a plate-plate

setup has been used. Such a setup is also known as PP. PP setup is right for linear viscoelastic materials but not suitable for nonlinear studies. It is also true that PP setup does not give a uniform shear rate throughout its geometry. In a PP setup, the samples are typically placed between the two at a gap of 1mm. This means that the samples are typically the size of 2 ml. Generally, two plate dimensions are used for measurements.

The shear at the edge of the plates is higher than the shear at the centre. This means that samples at the edge could dry out or have a different temperature when compared to the centre. This can be disadvantageous during temperature controlled/sensitive measurements. With samples such as bitumen, at high-temperature measurements, the sample can oxidise at the edges and effectively provide altered results. Similarly, gaps in the distance between the parallel plates (non-zero gap), particles lodged between the plates or damage to the surface can provide discrepancy to the results.

25 mm and 8 mm diameter plates were used in this thesis. The gap for measurements for a 25 mm plates is 1 mm and for 8 mm plates the gap is increased to 2 mm. The samples that are subjected to the test undergo shear between 100 Pa to 10 MPa during the test, and the temperature is varied to the desired range. In this thesis, the temperature was varied from 4° C to 88° C. The plates are made from stainless steel. Stainless steel is used as it has a low coefficient of thermal expansion and good heat-transfer coefficient. An environmental chamber is placed on top of the plates. This plate helps heat the sample at to the desired temperatures.

Measurements can be rotational or oscillatory. In an oscillation test, the top parallel plate oscillates with a predetermined frequency (angular deflection) or amplitude (torque). The amplitude or frequency depends on the material, with the primary focus being to keep the material within its linear viscoelastic region. For a material such as bitumen, the frequency of the oscillation test can vary between 1 to 160 rad/s and standard tests are performed at a fixed frequency of 10 rad/s. When sinusoidal stress is applied to a sample under oscillation, within its linear viscoelastic region, the material can respond to this with a response strain that is out of phase with the applied strain. This phase difference is called the phase angle. Thus, it is defined as the phase difference between the applied stress and strain. For a solid, the phase angle is 0° θ, and for a purely viscous liquid, it is 90° θ. Anywhere in between, the response is viscoelastic. The scientific representation of the oscillation test is displayed in Figure 4.8.

Geometrically speaking, the ratio of the resulting stress to the applied strain is called the complex shear modulus, G*.

$$G^* = G' + iG'' \tag{08}$$

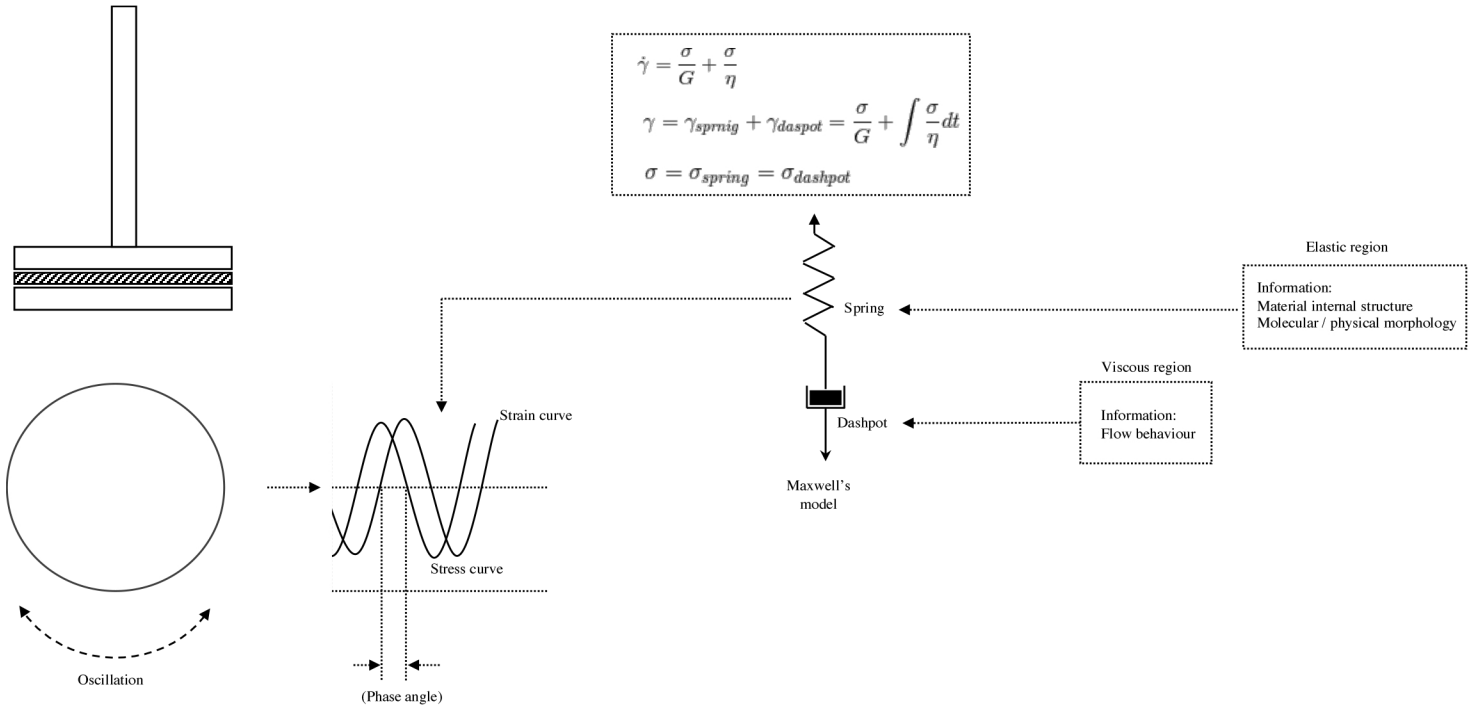

Figure 4.8, Schematic representation of the plate-plate setup. The stress to strain response from a DSR is in phase difference with each other. This behavior is best represented with Maxwell's model of viscoelasticity.

Once again, the in-phase component of complex shear modulus is called G' and the out-of-phase component is G''. The ratio of G' to G'' is called loss tangent.

$$tan(\delta) = \frac{G^{'}}{G^{''}} \tag{09}$$

The in-phase component is called storage modulus and is the cosine of the phase angle multiplied with the complex shear modulus

$$G^{'} = G^{*}cos(\delta) \tag{10}$$

and on the other hand, the out-of-phase component is called the loss modulus and it is defined as the sinusoidal component of the phase angle multiplied with the complex shear modulus.

$$G^{''} = G^{*}sin(\delta) \tag{11}$$

The storage modulus and loss modulus are not analogues to elastic and viscous components of the complex shear modulus but rather, both storage modulus, and loss modulus carry part of the elastic response. While loss modulus is the out of phase response, over time, the out of phase compound could also show delayed elastic response. Finally, the ratio of complex shear modulus to the angular frequency will provide the complex viscosity of the material.

$$\eta^{*} = \frac{G^{'} + iG^{''}}{\omega} \tag{12}$$

Similar to complex shear modulus, complex viscosity can be divided into real and imaginary components. The ratio of the storage modulus to the angular frequency provides the real component of the complex viscosity and the ratio of the loss modulus to the angular frequency provides the imaginary component of viscosity.

$$\eta^{*} = \eta^{'} + i\eta^{''} \tag{13}$$

5. Results and Conclusion

In the book 'The Big Picture: On the Origins of Life', Prof. Sean Carroll introduces the idea of poetic naturalism and elementalism. In the book, the author asks readers a profound philosophical question about human observation. He asks the readers to imagine a boat, over the years, the boat deteriorates, and its parts are replaced. At some point in the boat's life, all the components of the boat will be replaced by newer ones. This action raises a fundamental dilemma for a poetic naturalist. Somewhere in the world, there exist all the parts that were replaced. Hence if someone collected all those replaced parts and put them together, they end up with two boats with the same name and identification. On the other hand, this does not bother the Elementalist. Since the Elementalist claims that both the old and new boat, along with everything else in the observable universe is merely an arrangement of fundamental particles, this abstract thinking forces one to reduce all scientific question into simple systems of combinations of basic ideas, allowing the researcher to study complex question. This also allows researchers to extrapolate the results, be inspired by other fields of study and observe the bigger picture.

To carry out such observations of SARA systems. The behaviour of various subfractions must be observed individually and in tandem. Experiments were carried out in **papers 1 - 3** with this ideology. The results of these experiments will be observed with this attitude in tandem with the philosophical idea of double-negative observations, introduced in the previous chapter. Thus, the results of such an observation will provide a strong understanding of the SARA system and its interaction with dissimilar nanoparticles such as graphitic derivatives.

The techniques used in all the studies in this thesis can be categorised into microscopy, spectroscopy, diffraction, thermal analysis and rheology. DLS, DSR, SEM-EDX, FTIR, XRD, bright field imaging, and RTFOT. The characterisation techniques were selected based on its abilities to provide information about the behaviour of graphene derivatives, SARA system and the interaction between graphene derivatives and SARA system. For the validation of results, complementary techniques were used.

5.1. Results and discussion

5.1.1. Paper 1: Graphene derivative in SARA

In the paper **Induchoodan.G-2016** (unattached), the results helped conclude that graphene does indeed display an agglomeration pattern and that the chain length of the polymer can influence this behaviour. It is in contact with, and that the agglomeration behaviour is independent of extrinsic factors. This could mean that the agglomeration behaviour can be initiated by concentration. If true, the dominant

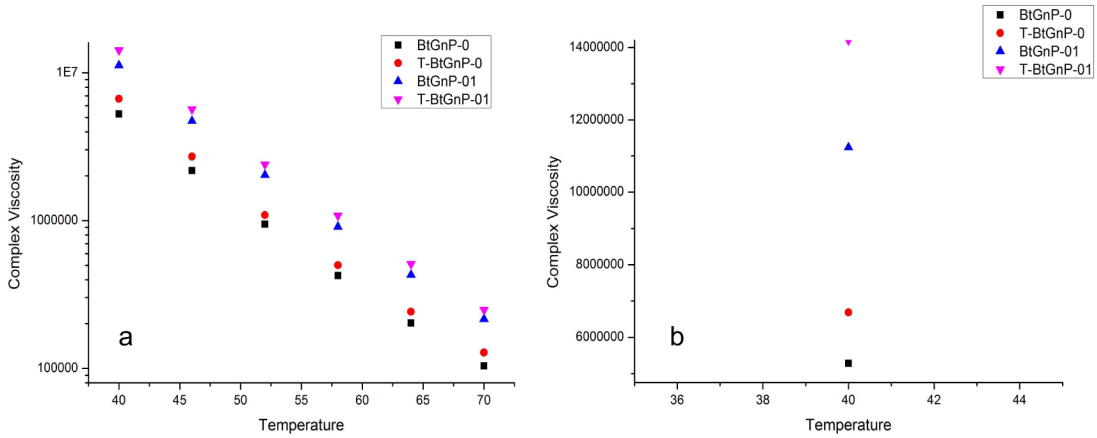

Figure 5.1: a). Log of complex viscosity vs temperature for neat binder and graphene embedded bitumen, before and after thermal oxidation. $\mathrm{BtGnP}-0$ and $\mathrm{T}-\mathrm{BtGnP}-0$ are neat binder before and after thermal oxidation and $\mathrm{T}-\mathrm{BtGnP}-0$ and $\mathrm{T}-\mathrm{BtGnP}-01$ are graphene embedded bitumen, before and after thermal oxidation. b) Complex viscosity vs temperature of neat binder and graphene embedded bitumen, before and after thermal oxidation, at 40°C.

question is as to whether this agglomeration tendency is dependent on the fractional concentration of graphene derivatives in SARA or the total concentration of all solid phases. If the latter is true, it raises the question of re-flocculation of the multiple phases.

The mesoscopic behaviour of graphene was indirectly observed in the paper. With 1% graphene, the experimental evidence displays an increase in the colloidal viscosity, see Figure 5.1. This is no surprise as the largest particles influence the colloidal viscosity in the sample. What is interesting is that the increase in viscosity supersedes expectations. Four samples were compared, i). SARA with graphene ii). SARA without graphene iii). thermally oxidised SARA and iv). thermally oxidised, graphene embedded SARA.

The shift in viscosity after thermal oxidation for samples with graphene was compositely larger than that for samples without graphene. It was evident from **Induchoodan.G-2016**, that graphene agglomerates as a factor of concentration and polymer chain length. This indicates a potential agglomeration behaviour in SARA with the introduction of graphitic derivatives. From the discrepancy increase in the rheological values of SARA with and without graphene, it can be inferred that the agglomeration is a factor of the total concentration of all solid phases in the system.

5.1.2. Paper 2: Graphene oxide in Synthetic SARA

SS3P SARA systems were tested for flocculation behaviour. GO SS3P systems successfully. The immediate results were that graphene derivatives such as GO causes immediate destabilisation of SS3P systems. This is in line with the predictions made in the previous two papers. The formation of micelles is similar to the prediction from literature. In this case, when GO is introduced to SS3P, there is an immediate

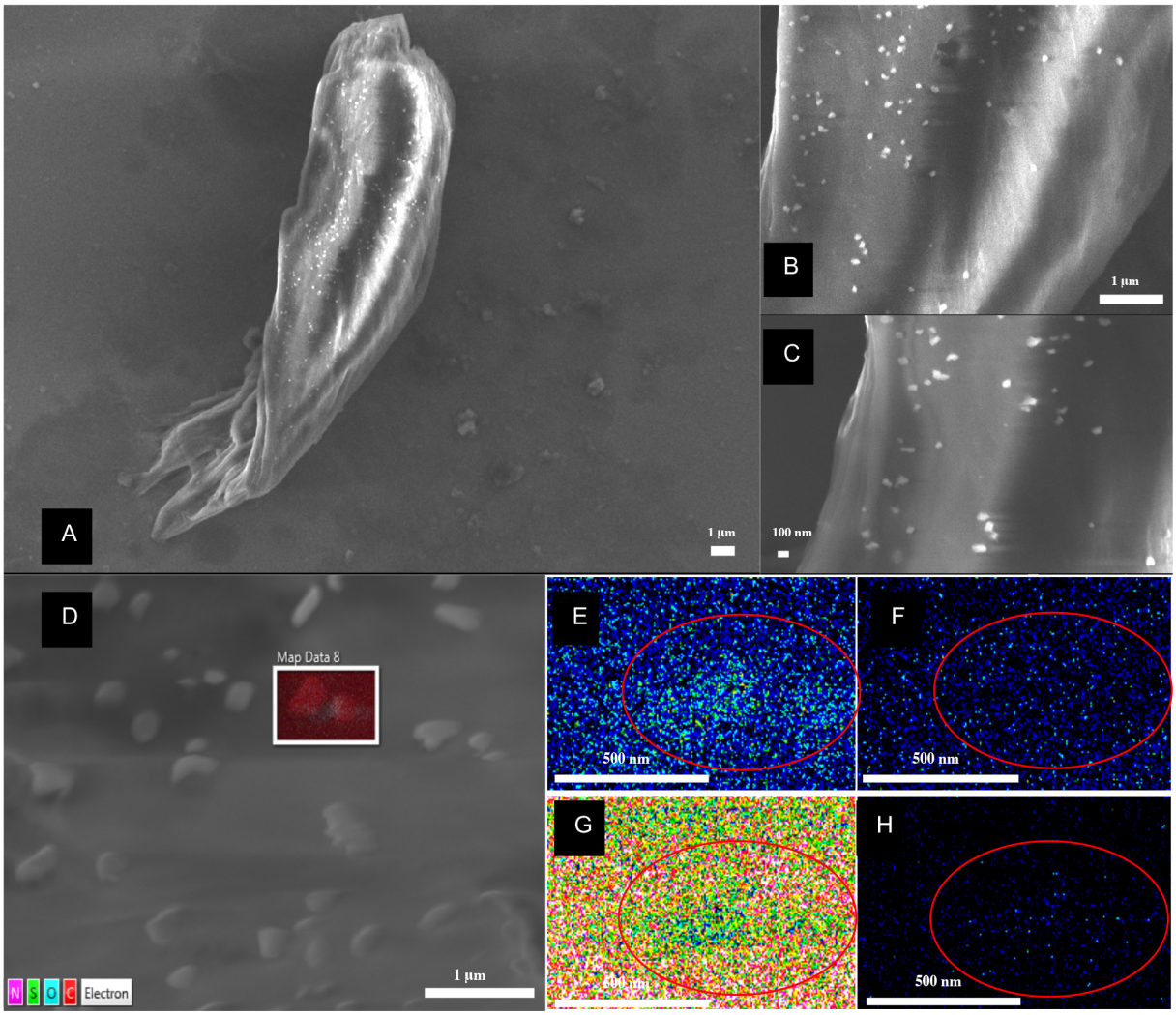

Figure 5.2: A). SEM image of an agglomerated structure of the precipitate. Asphaltene nanoparticles are seen to be adsorbed on the surface of GO. B&C). Zoomed in images of the agglomerate. D). EDX scan of the asphaltene precipitate. E). Oxygen peak F). Sulphur peaks G). Carbon peak H). Nitrogen peak.

disappearance of the micelle structures—leaving behind the alkane solvent—providing clear evidence of GO's effect on the colloidal microstructure.

Observations and results indicate that the introduction of GO into any subfraction of CODs that contain asphaltene would, in effect destabilise the structure of SARA. SS3P displayed spontaneous precipitation, followed by phase separation. From the results, we interpret that the phase separation caused by GO can be attributed to the oxygen groups that are found on GO.

SEM-EDX and XRD were performed on the precipitate. The results showed that the characterise 002-peak of asphaltene has broadened. This was an indication that the precipitate was amorphous. While the 002-peak was lost, the sample showed an aliphatic peak (Y-peak) and the characteristic 010-peak and 011-peak. From this, we could infer that the pattern was a combination of GO and asphaltene. To understand the morphology and chemical composition of the precipitate, we performed SEM-EDX. The images indicate that asphaltene has been absorbed on the surface of GO, see

Figure 5.2. Asphaltene has epitaxially self-arranged on top of GO. The elemental analysis gave distinct peaks for carbon, oxygen, nitrogen and sulphur. This helped confirm that the structure is indeed asphaltene.

Hence, All DBSA molecules have then been absorbed onto active sites on GO in the G-SS3P samples. A similar observation was made in Asphaltene-SS3P samples, to which GO was introduced. In SS3P, after the immediate phase separation, particles were found in the form of dispersant in the liquid phase. Upon interaction with these features, they immediately destabilised and sedimented. The results from interacting with the features helped us conclude that the structures found in SS3P are metastable. Finally, an interesting observation that was found was that GO-DBSA precipitates through flocculation, unlike all the other samples.

5.3.4. Paper 3: Functionalised graphene oxide in synthetic SARA

From the previous paper, we concluded that oxygen functional groups present on the surface of GO cause phase separation of colloidal and micelles asphaltene. To overcome the effect caused by the hydroxyl group, we functionalised GO. After functionalisation, the functional group replaced the hydroxyl group on the surface of GO. After dispersing fGO in SS3P, we could observe two main changes, when compared to GO. A new structure replaced the earlier asphaltene micelle. This novel micelle structure is attached to fGO (ensemble structure), see Figure 5.3. Secondly, NAs behave as co-surfactant to stabilise the ensemble structure. Having overcome the

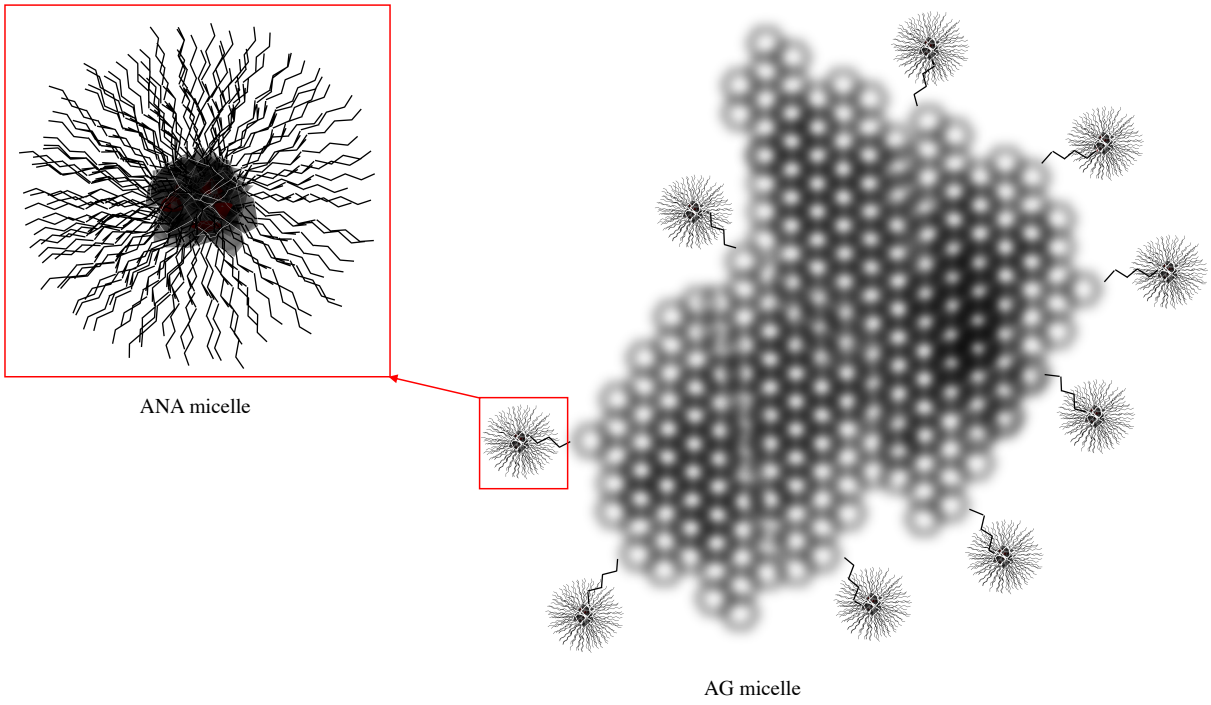

Figure. 5.3: Hypothesised structure of the ensemble structure. The structure is predicted to have a fGO core and NAs form micelles at the active sites.

question on stability, we focused on observing the structure of the micelles. We studied the system using a rotational rheometer, DLS, and SEM. At the first stage, we investigated the micelle structure with the help of rheology. Zero shear and viscosity run are some of the rheological techniques used in this study.

The rheological results lead to the conclusion that the high aspect ratio fGO ensemble structures showed patterns of reorientation of its ensemble structure. For low aspect ratio fGO ensemble structure and micelles formed by NAs, this pattern was not observed. From DLS measurements, we observed the size of the fGO ensemble structure and stability of this structure. Combined results from DLS, SEM and rotational rheometer helped us conclude that the fGO interaction is dependent on the number of active sites available on the surface of fGO. Thus, the aspect ratio of fGO and the number of active sites would determine the shape, stability and final shape. This shape could vary between sphere, rod or disk.

5.2. Additional results

GO was dispersed in SS2P systems successfully. The immediate results were that graphene derivatives such as GO causes immediate destabilisation of both SS2P. In SS2P, GO causes agglomeration of asphaltene colloids. Asphaltene-GO agglomerates are observed to precipitate at a prolonged rate over 12 hours. It was indicating a slow movement of the particles. The difference in rate and mechanism can be attributed to the difference between colloidal and micelles asphaltenes and the various intermolecular bonding that contributed to the dispersion of asphaltenes in SS2P and SS3P. Clusters were observed in SS2P samples after 12 hours, refer to Figure 5.4. These were found to be interesting. We interpret that the clusters observed in SS2P are asphaltene-GO agglomerates that have formed by the interaction between the two species.

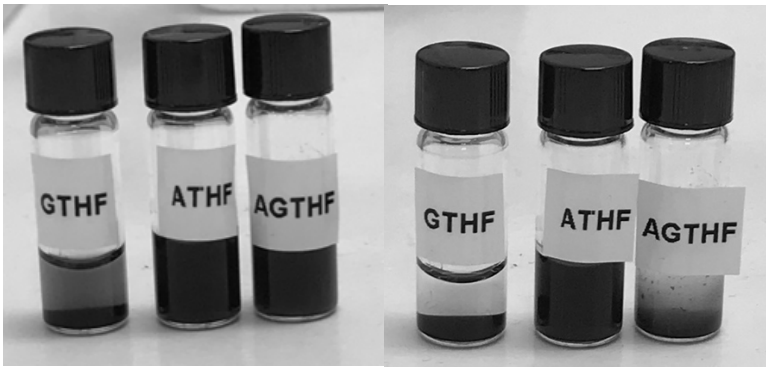

Figure. 5.4: SS2P samples of GO, asphaltene and GO + asphaltene in THF; Right: SS2P samples after 12 hours.

5.3. Conclusion

In this thesis, we introduced and investigated a previously ignored problem. While many researchers decided to investigate the property of the bulk, of the modified SARA systems, we took it upon us to understand the underlying interaction between the nanoparticles. This approach led us to realise that GO is highly detrimental to the structure of SARA. We used various characterisation techniques to prove this behaviour of GO in SARA. Later, we provided a solution to the problem by transforming the surface functional groups on GO. This modification helped us construct novel and stable graphitic structures in SARA.

6. Future Outlook

The road not taken is amongst the most misinterpreted literature works. In the poem, Robert Frost is in a conundrum with a choice to take one of many paths put forward to him. All choices are equally travelled, and as he says, the mistake is to not chose one.

Two roads diverged in a yellow wood,
And sorry I could not travel both
And be one traveller, long I stood
And looked down one as far as I could
To where it bent in the undergrowth

This is true for all research topics, and this thesis is no exception. Betwixt scientific pursuit, unanticipated questions pop in and out of existence. It becomes the choice of each researcher to seek such questions or staying on course with the primary question. In this research, such a choice had presented itself. During the inception of the thesis, the intent was to formulate a design protocol to improve the properties of bitumen. During the research, an interesting observation as the one presented in **paper 1** manifested itself. The choice was made to investigate the question before proceeding to answer the primary question.

Investigating the question leads to a series of 4 ongoing steps to observe agglomeration and flocculation in SARA systems. Heretofore, 3 of the 4 steps have been completed. They are presented as **papers 1-3**.

The proposed way forward after licentiate with this study is to isolate the variables in the synthetic SARA and study their contribution. The potential variables in the synthetic SARA are the chemical structure of asphaltene, size of nanoparticles and concentration. While size and concentration can be controlled and predicted for a realistic SARA, the chemical structure is less certain due to the vast possibilities of chemical architecture in asphaltene. Various asphaltenes can be extracted using SARA distillation and characterised using mass spectroscopy (MS). By doing so, it will provide a clear and direct understanding of the structure and potential bonds that can be formed during the interaction between asphaltene and GO. This approach is demanding in terms of time and resources due to the complexity of the approach. Thus, it can be proposed that this approach remain secondary.

Another way forward instead of selecting different asphaltenes is that GO can be functionalised with various end functional groups while using the same asphaltene (maintaining the chemical architecture). Firstly, the structure of the micelles will be studied. Following this, the structural changes in GO will be investigated. After the

structure is understood, GO will be end functionalised with the aim to form stable structures with asphaltene and resins. Eventually, after the structure is established, its impact on material function will be studied and displayed. XRD, FTIR and Raman will be used to study the structure of chemical architecture of asphaltene, graphene derivatives and functionalised GO. SAXS will be used as a primary technique to study the micelles, stability of synthetic SARA. MS will be utilised in the beginning to establish the chemical composition of the asphaltene used in the study after licentiate. Simultaneously, asphaltene samples will be characterised with the help of an external lab to establish the various chemical architectures. In the end, the structure of the micelles, the potential bonds, chemical architecture of asphaltene and GO will be used to provide a clear understanding of whether graphene derivatives are causing a universal phase separation or if certain functional groups can avoid it.

Acknowledgement

In India, we believe in the proverb *Matha Pitha Guru Deivam.* When translated, it means your mother is your first teacher, followed by your father. Then comes your teacher and finally comes God. That is the order in which I would like to acknowledge. I wish to begin by thanking my **parents,** who believed that their children are their most significant assets in life. None of this would have been possible without the two of you. I also wish to thank my **brother**, who has been my biggest competition, you help me grow. I want to thank the spirits of my grandparents. I know that you are not here to see my progress in life, but I wish to tell you that I can feel your blessings in every step I take in life.

After Matha and Pitha, comes Guru. Dear **Jan**, I would like to begin by thanking you. You are a great mentor. You have saved and supported me in the toughest of times, and I'm ever so grateful to you for being there for me. I know that I'm learning to be a better researcher every day, and as someone who has reached great heights, it must be a demanding task to raise me to your level. Sorry and thank you for that.

Eva, you too choose to support and raise me when I needed it the most, and I'm ever so grateful to you and in your debt for supporting me. Thank you!

My friends, Ceci, Mohanna, Kengo, Pierre, Bobby, and Alex; we are all idiots travelling in the same boat called insanity. I love all you idiots for being there for me. Lorenzo and Denis, you guys, are amongst those few friends that I meet one a year but think about throughout the year. Lorenzo, sometimes I wonder what life would have been if I never met you. I would like to take this opportunity to thank Emma; you were my first support and friend when I started my PhD. Erik, Mattias and Karin, our politically incorrect definitely confusing and scary conversation have helped me a lot in developing myself as a better human. Karin, especially you! I never knew the problems of Pony land before I met you. Inna, thank you for all those lunch conversations and the times I got to barge into your office with silly doubts. Elina, I want to thank you for your encouragement and excitement every time I talk about work at non work times.

NPRA, I do not think I could have had an opportunity to write this kappa if you did not fund me. Helen, Amir, Marek, Peter, Per and Britt-Marie, thank you all for helping me at various stages in my research. Every support that I got from you was like a brick that helped me built myself as a researcher. I wish to thank all my colleagues in Nano and Biophysics and namely my group members in BioLab. Lastly, I want to thank my nemesis, ''Kitty''. You have been my companion from school days.

References

[1]. Frenking, G. and Shaik, S., 2014. The Chemical Bond: Fundamental Aspects of Chemical Bonding. 1st ed. Wiley Online Library.

[2]. Jindal, U., 2012. Material Science and Metallurgy. 1st ed. New Delhi: Dorling Kindersley.

[3]. Elton, D., Boukouvalas, Z., Butrico, M., Fuge, M. and Chung, P., 2018. Applying machine learning techniques to predict the properties of energetic materials. Scientific Reports, 8(1).

[4]. Kostorz, G., 2001. Phase Transformations in Materials. 1st ed. Wiley-VCH Verlag GmbH, pp.409-480.

[5]. Lin, Z., Zhang, H. and Yang, Y. (1999). Spinodal decomposition kinetics of a mixture of liquid crystals and polymers. Macromolecular Chemistry and Physics, 200(5), pp.943-948.

[6]. Crick,F. 1988. What Mad Pursuit, a Personal View of Scientific Discovery, Basic Books. (book)

[7]. Huttenhower, C. and Gevers, D., 2012. Structure, function and diversity of the healthy human microbiome. Nature, 486(7402), pp.207-214.

[8]. Yoo, B., Shin, H., Yoon, H. and Park, H., 2013. Graphene and graphene oxide and their uses in barrier polymers. Journal of Applied Polymer Science, 131(1),

[9]. Petrauskas, D. And Ullah,S. 2015, Manufacture and storage of bitumen, Shell handbook, Sixth Edition, Shell bitumen. (book)

[10]. Gruse, W.A. and Stevens, D.R. 1960. The Chemical Technology of Petroleum. McGraw-Hill. (book)

[11]. Çadýrcý, B., Abed, R., Abraham, W., Abraham, W., Adams, J., Aitken, C., Aitken, C., Al-Halbouni, D., Al-ramahi, Y., Alazard, D. and Albertin, K., 2011. Handbook of Hydrocarbon and Lipid Microbiology. Heidelberg, Germany: Springer-Verlag Berlin Heidelberg. (book)

[12]. Sciencedirect.com. 2020. Hydrocarbon - An Overview | Sciencedirect Topics. [online] Available at: <https://www.sciencedirect.com/topics/chemical-engineering/hydrocarbon> [Accessed 20 April 2020].

[13]. Nalinakshan, S., Sivasubramanian, V., Ravi, V., Vasudevan, A., Sankar, M. and Arunachalam, K., 2019. Progressive crude oil distillation: An energy-efficient alternative to conventional distillation process. Fuel, 239, pp.1331-1337.

[14]. Severin, D., 1992. Characterization of high- and non-boiling crude oil fractions. Invited lecture. The Analyst, 117(3), p.305.

[15]. George A. Olah and Árpád Molnár. 2003. Hydrocarbon Chemistry, Second Edition. Wiley & Sons. (book)

[16]. Gary JH, Handwerk GE, Kaiser MJ. 2007. Petroleum Refining: Technology and Economics. CRCPress. (book)

[17]. James G. Speight. 2015. Handbook of Coal Analysis, First Edition. Wiley & Sons. (book)

[18]. D4124-09. 2018. Standard Test Method for Separation of Asphalt into Four Fractions. ASTM international

[19]. Corbett, L., 1969. Composition of asphalt based on generic fractionation, using solvent deasphaltening, elution-adsorption chromatography, and densimetric characterization. Analytical Chemistry, 41(4), pp.576-579.
[20]. Ruiz-Morales, Y. and Mullins, O. (2007). Polycyclic Aromatic Hydrocarbons of Asphaltenes Analyzed by Molecular Orbital Calculations with Optical Spectroscopy. Energy & Fuels, 21(1), pp.256-265.
[21]. Handle, F., Harir, M., Füssl, J., Koyun, A., Grossegger, D., Hertkorn, N., Eberhardsteiner, L., Hofko, B., Hospodka, M., Blab, R., Schmitt-Kopplin, P. and Grothe, H. (2017). Tracking Aging of Bitumen and Its Saturate, Aromatic, Resin, and Asphaltene Fractions Using High-Field Fourier Transform Ion Cyclotron Resonance Mass Spectrometry. Energy & Fuels, 31(5), pp.4771-4779.
[22]. Lesueur, D. (2009). The colloidal structure of bitumen: Consequences on the rheology and on the mechanisms of bitumen modification. Advances in Colloid and Interface Science, 145(1-2), pp.42-82.
[23]. Subramanian, S., Simon, S. and Sjöblom, J. (2015). Asphaltene Precipitation Models: A Review. Journal of Dispersion Science and Technology, 37(7), pp.1027-1049.
[24]. Richardson, C., 1905. The Modern Asphalt Pavement, 2nd ed. J. Wiley & sons.
[25]. Nellensteyn, F., 1924. The constitution of asphalt. Journal of the Institution of Petroleum Technologists, 10, pp.311-315.
[26]. Pfeiffer, J. and Saal, R., 1940. Asphaltic Bitumen as Colloid System. The Journal of Physical Chemistry, 44(2), pp.139-149.
[27]. Saal, R. and Labout, J., 1940. Rheological Properties of Asphaltic Bitumen. The Journal of Physical Chemistry, 44(2), pp.149-165.
[28]. Dickie, J. and Yen, T., 1967. Macrostructures of the asphaltic fractions by various instrumental methods. Analytical Chemistry, 39(14), pp.1847-1852.
[29]. Mullins, O. (2011). Asphaltenes, heavy oils, and petroleomics. New York: Springer. (book)
[30]. Draude, A. and Dierking, I. (2019). Lyotropic Liquid Crystals from Colloidal Suspensions of Graphene Oxide. Crystals, 9(9), p.455.
[31]. Li, P., Wong, M., Zhang, X., Yao, H., Ishige, R., Takahara, A., Miyamoto, M., Nishimura, R. and Sue, H. (2014). Tunable Lyotropic Photonic Liquid Crystal Based on Graphene Oxide. ACS Photonics, 1(1), pp.79-86.
[32]. Kim, D., Lim, S., Jung, D., Hwang, J., Kim, N. and Jeong, K. (2017). Self-assembly and polymer-stabilization of lyotropic liquid crystals in aqueous and non-aqueous solutions. Liquid Crystals Reviews, 5(1), pp.34-52.
[33]. Alhreez, M. and Wen, D. (2019). Molecular structure characterization of asphaltene in the presence of inhibitors with nanoemulsions. RSC Advances, 9(34), pp.19560-19570.
[34]. Liu, J., Li, X., Jia, W., Li, Z., Zhao, Y. and Ren, S. (2015). Demulsification of Crude Oil-in-Water Emulsions Driven by Graphene Oxide Nanosheets. Energy & Fuels, 29(7), pp.4644-4653.
[35]. Pérez, E. and Martín, N., 2015. π–π interactions in carbon nanostructures. Chemical Society Reviews, 44(18), pp.6425-6433.

[36]. Wang, J., Chen, Z. and Chen, B., 2014. Adsorption of Polycyclic Aromatic Hydrocarbons by Graphene and Graphene Oxide Nanosheets. Environmental Science & Technology, 48(9), pp.4817-4825.
[37]. Cimino, R., Rasmussen, C., Brun, Y. and Neimark, A., 2016. Mechanisms of chain adsorption on porous substrates and critical conditions of polymer chromatography. Journal of Colloid and Interface Science, 481, pp.181-193.
[38]. Nguyen, L. and Truong, T. (2018). Quantitative Structure–Property Relationships for the Electronic Properties of Polycyclic Aromatic Hydrocarbons. ACS Omega, 3(8), pp.8913-8922.
[39]. Andreatta, G., Bostrom, N. and Mullins, O., 2005. High-QUltrasonic Determination of the Critical Nanoaggregate Concentration of Asphaltenes and the Critical Micelle Concentration of Standard Surfactants. Langmuir, 21(7), pp.2728-2736.
[40]. Abdel-Raouf, M. (2012). Crude Oil Emulsions- Composition Stability and Characterization. 1st ed. InTech. (Book)
[41]. Andersen, S. and Christensen, S. (2000). The Critical Micelle Concentration of Asphaltenes As Measured by Calorimetry. Energy & Fuels, 14(1), pp.38-42.
[42]. Ashoori, S., Sharifi, M., Masoumi, M. and Mohammad Salehi, M. (2017). The relationship between SARA fractions and crude oil stability. Egyptian Journal of Petroleum, 26(1), pp.209-213.
[43]. Polymer flocculation, principles and applications. (1973). Melbourne: Royal Australian Chemical Institute (Victorian Branch). (Book)
[44]. Geim, A. and Novoselov, K., 2007. The rise of graphene. Nature Materials, 6(3), pp.183-191.
[45]. Li, X., Li, B., Fan, X., Wei, L., Li, L., Tao, R., Zhang, X., Zhang, H., Zhang, Q., Zhu, H., Zhang, S., Zhang, Z. and Zeng, C., 2018. Atomically flat and thermally stable graphene on Si (111) with preserved intrinsic electronic properties. Nanoscale, 10(18), pp.8377-8384.
[46]. Gudarzi, M. (2016). Colloidal Stability of Graphene Oxide: Aggregation in Two Dimensions. Langmuir, 32(20), pp.5058-5068.
[47]. Castro Neto, A., Guinea, F., Peres, N., Novoselov, K. and Geim, A. (2009). The electronic properties of graphene. Reviews of Modern Physics, 81(1), pp.109-162.
[48]. Gioia, L., Zülicke, U., Governale, M. and Winkler, R., 2018. Dirac electrons in quantum rings. Physical Review B, 97(20).
[49]. Novoselov, K., Geim, A., Morozov, S., Jiang, D., Katsnelson, M., Grigorieva, I., Dubonos, S. and Firsov, A., 2005. Two-dimensional gas of massless Dirac fermions in graphene. Nature, 438(7065), pp.197-200.
[50]. Jiang, Z., Zhang, Y., Tan, Y., Stormer, H. and Kim, P., 2007. Quantum Hall effect in graphene. Solid State Communications, 143(1-2), pp.14-19.
[51]. Morozov, S., Novoselov, K., Katsnelson, M., Schedin, F., Ponomarenko, L., Jiang, D. and Geim, A., 2006. Strong Suppression of Weak Localization in Graphene. Physical Review Letters, 97(1).

[52]. Baringhaus, J., Ruan, M., Edler, F., Tejeda, A., Sicot, M., Taleb-Ibrahimi, A., Li, A., Jiang, Z., Conrad, E., Berger, C., Tegenkamp, C. and de Heer, W., 2014. Exceptional ballistic transport in epitaxial graphene nanoribbons. Nature, 506(7488), pp.349-354.

[53]. Partoens, B. and Peeters, F., 2006. From graphene to graphite: Electronic structure around the K point. Physical Review B, 74(7).

[54]. De Leo, F., Magistrato, A. and Bonifazi, D., 2015. Interfacing proteins with graphitic nanomaterials: from spontaneous attraction to tailored assemblies. Chemical Society Reviews, 44(19), pp.6916-6953.

[55]. Randviir, E., Brownson, D. and Banks, C., 2014. A decade of graphene research: production, applications and outlook. Materials Today, 17(9), pp.426-432.

[56]. Zhu, S., Yuan, S. and Janssen, G. (2014). Optical transmittance of multilayer graphene. EPL (Europhysics Letters), 108(1), p.17007.

[57]. Skoda, M., Dudek, I., Jarosz, A. and Szukiewicz, D., 2014. Graphene: One Material, Many Possibilities—Application Difficulties in Biological Systems. Journal of Nanomaterials, 2014, pp.1-11.

[58]. Inagaki, M. and Kang, F., 2014. Graphene derivatives: graphane, fluorographene, graphene oxide, graphyne and graphdiyne. J. Mater. Chem. A, 2(33), pp.13193-13206.

[59]. Inc., C., 2020. Understanding Graphene Nanoplatelets. [online] AZoNano.com. Available at: <https://www.azonano.com/article.aspx?ArticleID=4846> [Accessed 20 April 2020].

[60]. Dreyer, D., Park, S., Bielawski, C. and Ruoff, R., 2010. The chemistry of graphene oxide. Chem. Soc. Rev., 39(1), pp.228-240.

[61]. Schultz, B., Dennis, R., Lee, V. and Banerjee, S., 2014. An electronic structure perspective of graphene interfaces. Nanoscale, 6(7), p.3444.

[62]. Szabó, T., Berkesi, O., Forgó, P., Josepovits, K., Sanakis, Y., Petridis, D. and Dékány, I., 2006. Evolution of Surface Functional Groups in a Series of Progressively Oxidized Graphite Oxides. Chemistry of Materials, 18(11), pp.2740-2749.

[63]. Oye, M. (2013). Graphene Synthesis and Applications (Choi, W. and Lee, J.-W., Eds.) [Book Review]. IEEE Nanotechnology Magazine, 7(1), pp.39-40.

[64]. Mahalingam, D., Wang, S. and Nunes, S. (2018). Graphene Oxide Liquid Crystal Membranes in Protic Ionic Liquid for Nanofiltration. ACS Applied Nano Materials, 1(9), pp.4661-4670.

[65]. Hernandez, Y., Lotya, M., Rickard, D., Bergin, S. and Coleman, J. (2010). Measurement of Multicomponent Solubility Parameters for Graphene Facilitates Solvent Discovery. Langmuir, 26(5), pp.3208-3213.

[66]. Liu, J., Tang, J. and Gooding, J., 2012. Strategies for chemical modification of graphene and applications of chemically modified graphene. Journal of Materials Chemistry, 22(25), p.12435.

[67]. Georgakilas, V., Otyepka, M., Bourlinos, A., Chandra, V., Kim, N., Kemp, K., Hobza, P., Zboril, R. and Kim, K. (2012). Functionalization of Graphene:

Covalent and Non-Covalent Approaches, Derivatives and Applications. Chemical Reviews, 112(11), pp.6156-6214.
[68]. Habte, A. and Ayele, D. (2019). Synthesis and Characterization of Reduced Graphene Oxide (rGO) Started from Graphene Oxide (GO) Using the Tour Method with Different Parameters. Advances in Materials Science and Engineering, 2019, pp.1-9.
[69]. Motalo, V., 2019. ANALYSIS OF VERIFICATION AND CALIBRATION METHODOLOGIES OF MEASURING INSTRUMENTS. Measuring Equipment and Metrology, 80(1), pp.51-66.
[70]. Price, D., 1995. Temperature calibration of differential scanning calorimeters. Journal of Thermal Analysis, 45(6), pp.1285-1296.
[71]. Allen, A., Zhang, F., Kline, R., Guthrie, W. and Ilavsky, J., 2017. NIST Standard Reference Material 3600: Absolute Intensity Calibration Standard for Small-Angle X-ray Scattering. Journal of Applied Crystallography, 50(2), pp.462-474.
[72]. Francis, G. and Humphreys, I., 2005. Benchmarking an International Journal. Bradford, England: Emerald Group Publishing. (book)
[73]. Little, James L. (2011). "Identification of "known unknowns" utilizing accurate mass data and ChemSpider". Journal of the American Society for Mass Spectrometry. 23 (1): 179–185.
[74]. Dimiev, A. and Eigler, S., n.d. Graphene Oxide: Fundamentals and Applications. 1st ed. Wiley Online Library, pp.85-164. (book)
[75]. Yuan, C., Varfolomeev, M., Emelianov, D., Eskin, A., Nagrimanov, R., Kok, M., Afanasiev, I., Fedorchenko, G. and Kopylova, E., 2017. Oxidation Behavior of Light Crude Oil and Its SARA Fractions Characterized by TG and DSC Techniques: Differences and Connections. Energy & Fuels, 32(1), pp.801-808.
[76]. Priyanto, S., Mansoori, G. and Suwono, A. (2001). Measurement of property relationships of nano-structure micelles and coacervates of asphaltene in a pure solvent. *Chemical Engineering Science*, 56(24), pp.6933-6939.
[77]. Buenrostro-Gonzalez, E., Lira-Galeana, C., Gil-Villegas, A. and Wu, J. (2004). Asphaltene precipitation in crude oils: Theory and experiments. AIChE Journal, 50(10), pp.2552-2570.
[78]. Natarajan, A., Xie, J., Wang, S., Masliyah, J., Zeng, H. and Xu, Z. (2011). Understanding Molecular Interactions of Asphaltenes in Organic Solvents Using a Surface Force Apparatus. *The Journal of Physical Chemistry C*, 115(32), pp.16043-16051.
[79]. Konios, D., Stylianakis, M., Stratakis, E. and Kymakis, E., 2014. Dispersion behaviour of graphene oxide and reduced graphene oxide. *Journal of Colloid and Interface Science*, 430, pp.108-112.
[80]. Us'yarov, O., 2020. Critical Micellization Concentration of Ionic Surfactants: Comparison of Theoretical and Experimental Results.
[81]. Larichev, Y., Nartova, A. and Martyanov, O. (2016). The influence of different organic solvents on the size and shape of asphaltene aggregates studied via small-angle X-ray scattering and scanning tunneling microscopy. Adsorption Science & Technology, 34(2-3), pp.244-257.

[82]. Fletcher, P., 1996. Self-assembly of micelles and microemulsions. Current Opinion in Colloid & Interface Science, 1(1), pp.101-106.
[83]. Schafheutle, M. and Finkelmann, H., 1988. Shapes of Micelles and Molecular Geometry Synthesis and Studies on the Phase Behaviour, Surface Tension and Rheology of Rigid Rod-Like Surfactants in Aqueous Solutions. Liquid Crystals, 3(10), pp.1369-1386.
[84]. Chang, C. and Fogler, H. (1994). Stabilization of Asphaltenes in Aliphatic Solvents Using Alkylbenzene-Derived Amphiphiles. 1. Effect of the Chemical Structure of Amphiphiles on Asphaltene Stabilization. Langmuir, 10(6), pp.1749-1757.
[85]. Goual, L. and Sedghi, M., 2015. Role of ion-pair interactions on asphaltene stabilization by alkylbenzenesulfonic acids. Journal of Colloid and Interface Science, 440, pp.23-31.
[86]. Sato, T., Araki, S., Morimoto, M., Tanaka, R. and Yamamoto, H. (2014). Comparison of Hansen Solubility Parameter of Asphaltenes Extracted from Bitumen Produced in Different Geographical Regions. Energy & Fuels, 28(2), pp.891-897.
[87]. Konios, D., Stylianakis, M., Stratakis, E. and Kymakis, E., 2014. Dispersion behaviour of graphene oxide and reduced graphene oxide. Journal of Colloid and Interface Science, 430, pp.108-112.
[88]. Painter, P., Veytsman, B. and Youtcheff, J., 2015. Guide to Asphaltene Solubility. Energy & Fuels, 29(5), pp.2951-2961.
[89]. Hummers, W. and Offeman, R., 1958. Preparation of Graphitic Oxide. Journal of the American Chemical Society, 80(6), pp.1339-1339.
[90]. Olivieri, A., 2014. Analytical Figures of Merit: From Univariate to Multiway Calibration. Chemical Reviews, 114(10), pp.5358-5378.
[91]. Busse, R., Scacioc, A., Hernandez, J., Krick, R., Stephan, M., Janshoff, A., Thumm, M. and Kühnel, K., 2013. Qualitative and quantitative characterization of protein-phosphoinositide interactions with liposome-based methods. Autophagy, 9(5), pp.770-777.
[92]. Murphy, D. and Davidson, M., 2013. Fundamentals of Light Microscopy and Electronic Imaging. Hoboken, N.J.: Wiley-Blackwell. (book)
[93]. Reimer, L., 2013. Transmission Electron Microscopy. Berlin, Heidelberg: Springer Berlin / Heidelberg. (book)
[94]. Choudhary, O. and ka, P., 2017. Scanning Electron Microscope: Advantages and Disadvantages in Imaging Components. International Journal of Current Microbiology and Applied Sciences, 6(5), pp.1877-1882.
[95]. Corset, J. and Turrell, G., 2003. Raman Microscopy. Amsterdam: Academic Press. (book)
[96]. Stuart, B., 2009. Infrared Spectroscopy: Fundamentals and Applications. 1st ed. J. Wiley & Sons.
[97]. Hernandez, V., Ramirez, F., Zotti, G. and López Navarrete, J., 1992. Resonance Raman and FTIR spectra of pristine and doped polyconjugated polyfuran. Chemical Physics Letters, 191(5), pp.419-422.

[98]. Polavarapu, P., 1998. Vibrational Spectra: Principles and Applications with Emphasis on Optical Activity, Volume 85. 1st ed. Elsevier.
[99]. Levine, S., Li-Shi, Y., Strang, C. and Hong-Kui, X., 1989. Advantages and Disadvantages in the Use of Fourier Transform Infrared (FTIR) and Filter Infrared (FIR) Spectrometers for Monitoring Airborne Gases and Vapors of Industrial Hygiene Concern. Applied Industrial Hygiene, 4(7), pp.180-187.
[100]. Waseda, Y., Matsubara, E. and Shinoda, K., 2014. X-Ray Diffraction Crystallography. Berlin: Springer Berlin. (book)
[101]. Hammond, C., 2015. The Basics of Crystallography and Diffraction. 4th ed. Oxford: Oxford University Press. (book)
[102]. Feshbach, H., 1951. Elastic Scattering of Electrons. Physical Review, 84(6), pp.1206-1210.
[103]. Pecharsky, V. and Zavalij, P., 2009. Fundamentals of Powder Diffraction and Structural Characterization of Materials. New York: Springer. (book)
[104]. Barnes, H., Hutton, J. and Walters, K., 1989. An Introduction to Rheology. Amsterdam: Elsevier. (book)
[105]. Macosko, C., 1994. Rheology: Principles, Measurements, and Applications. New York, N.Y. etc.: Wiley-VCH. (book)
[106]. Barnes, H., 2000. A Handbook of Elementary Rheology. Aberystwyth: Institute of non-newtonian fluid mechanics, University of Wales. (book)

Summary

In predictive science, it is essential to understand the structure of a system under study to predict the behaviour arcuately. This means comprehending a structure-function relationship in a system, through understanding the underlying mechanism, governing principles, origin and evolution of the system. This was famously coined by Francis Crick in his axiom, ‘’If you want to understand the function, study the structure’’. From the aim of this thesis, this means that the structure-function and the underlying working principles of the parent material must be established. An excellent example of this theory is the human hand. The fist may be multifunctional, but its primary functions are for fine-controls and power movement. The structure of an opposing thumb makes fine-controls possible and the ability of the fingers to touch the thumb makes grabbing possible, and though this, power movements. On a molecular scale, the chemical structure of the molecule determines its properties and the properties of the molecules determine its function.

In this thesis, the structure of the molecules in bitumen will be investigated, in order to be able to determine its function. Through this, a predict will be made regarding the enhanceablity of the structure to attain the intended function and the potential for graphitic derivatives in this pursuit. It is possible to perform such a study on all the molecular families in bitumen; in reality, this would be a colonial undertaking that would be complex on an engineering scale. Instead, bitumen is for what it is, an engineering synonym for SARA. SARA is a complex polymeric colloidal solution with carbon, hydrogen and heteroatoms forming all possible chemical structures their free energy permits.

Starting with the modified Yen model as a foundation, the interaction between asphaltenes and graphene derivatives will be studied in natural and synthetic environments, to be able to understand the agglomeration tendencies and colloidal stably. Besides natural SARA, two synthetic systems were created. SS2P, a two-phase system of asphaltene nano agglomerate in solvent and 3 phase micelle system called SS3P with alkanes, resins and asphaltene. Graphene derivatives were allowed to interact with all 3 systems. DLS, XRD, FTIR, SEM, Rheology, TLC-FID, will be used in this attempt to understand their behaviour. The characterisation techniques and methods developed in the thesis are part of a greater attempt to satisfy the burden of proof bestrode upon on the researchers, in their attempt to answer the possibility of manipulating the properties of SARA. This research was initiated to help answer the global need for advanced materials to better society.